International Journal of Applied Earth Observation and Geoinformation 142 (2025) 104704

Contents lists available at ScienceDirect

International Journal of Applied Earth Observation and Geoinformation

journal homepage: www.elsevier.com/locate/jag

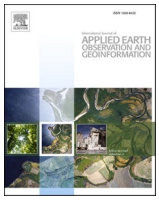

Quantifying the functional composition and potential resilience hotspots across a large latitudinal and environmental gradient in South American forests

Xiongjie Deng [a,*], Danny E. Carvajal [b,c], Rocío Urrutia-Jalabert [d,e,f,g], Waira S. Machida [h], Alice Rosen [a,i], Huanyuan Zhang-Zheng [a,j], David Galbraith [k], Sandra Díaz [l,m], Yadvinder Malhi [a,j], Jesús Aguirre-Gutiérrez [a,j]

[a] Environmental Change Institute, School of Geography and the Environment, University of Oxford, Oxford, UK
[b] Departamento de Biología, Universidad de La Serena, Casilla 554, La Serena, Chile
[c] Instituto de Ecología y Biodiversidad (IEB), Santiago, Chile
[d] Facultad de Ciencias Agropecuarias y Medioambiente, Universidad de la Frontera, Temuco, Chile
[e] Millennium Nucleus of Patagonian limit of Life (LiLi), Chile
[f] Center for Climate and Resilience Research CR2, Santiago, Chile
[g] Instituto de Conservación Biodiversidad y Territorio, Facultad de Ciencias Forestales y Recursos Naturales, Universidad Austral de Chile, Valdivia, Chile
[h] Departamento de Ecologia, Instituto de Ciências Biológicas, Universidade Federal de Goiás, Brasil
[i] Department of Biology, University of Oxford, Oxford, UK
[j] Leverhulme Centre for Nature Recovery, University of Oxford, Oxford, UK
[k] School of Geography, University of Leeds, Leeds, UK
[l] Consejo Nacional de investigaciones Científicas y Técnicas, Instituto Multidisciplinario de Biología Vegetal (IMBIV), Córdoba, Argentina
[m] Facultad de Ciencias Exactas, Físicas y Naturales, Universidad Nacional de Córdoba, Córdoba, Argentina

ARTICLE INFO

Keywords:
Remote sensing
Functional traits
Functional diversity
Functional redundancy
Temperate forests
Trait-environment relationships

ABSTRACT

Accurately inferring plant functional trait composition, diversity, and redundancy across space and time is pivotal for understanding environmental change impacts on forests' biodiversity and functioning. Here, we tested the capabilities of combining *in-situ* and remote sensing approaches to deliver accurate estimates of functional trait composition, diversity, and redundancy of temperate forest vegetation in South America (30°S to 53°S) considering leaf and stem morphological, nutrient, hydraulic, and photosynthetic traits. We identified hydrological stress, soil properties, and topography as key drivers of plant functional trait distribution and variation. Further, hydrological stress and soil properties were key determinants of functional diversity and redundancy across a large latitudinal gradient. Functional diversity peaked across Mediterranean forests, occupying between 30°S to 35°S. Functional diversity and redundancy were both high at latitudes between 35°S and 42°S, coinciding with Valdivian rainforests. Conversely, functional redundancy peaked between 42°S and 48°S, corresponding to Austral forests. Towards the southernmost extent of the study area, functional diversity and redundancy were both low between 48°S and 53°S, corresponding to the Magellanic subpolar forests. Our results highlight areas in South American temperate forests where both plant functional diversity and redundancy were maximal, hence potentially pointing towards areas more resilient to environmental change.

1. Introduction

Temperate forests show remarkable diversity in terms of species, soil composition, and the carbon dynamics within their ecosystems (Malhi et al., 2024, Malhi et al., 1999). In particular, due to their geographic isolation, temperate forests in Chile are highly endemic at species and higher taxonomic levels (Smith-Ramírez, 2004), and thus have become a priority for conservation (Echeverría et al., 2006). These temperate forests also provide essential contributions to people (Isbell et al., 2017), protecting watersheds, and absorbing and storing large amounts of carbon (Chen et al., 2023; Perez-Quezada et al., 2021; Urrutia-Jalabert et al., 2015a; Urrutia-Jalabert et al., 2015b). These forests therefore

* Corresponding author.
E-mail address: xiongjie.deng@ouce.ox.ac.uk (X. Deng).

https://doi.org/10.1016/j.jag.2025.104704
Received 20 March 2025; Received in revised form 26 June 2025; Accepted 26 June 2025
Available online 1 July 2025

contribute to long-term carbon sequestration (Oliver et al., 2015) and further influence temperature, humidity, and precipitation patterns (Ellis and Eaton, 2021). However, these forests are under persistent threat from replacement by other land covers and uses, such as crops and exotic plantations, degradation (Echeverría et al., 2006), unsustainable logging, warming, and precipitation decrease (Miranda et al., 2017; Perez-Quezada et al., 2023; Urrutia-Jalabert et al., 2015a; Urrutia-Jalabert et al., 2015b). As a result, the interactions that underpin ecosystem functions and benefits to people have become progressively fragile (Donohue et al., 2016). Therefore, it is essential to understand how ecosystem functioning and biodiversity vary across environmental gradients and respond to key environmental drivers in such temperate forests. This knowledge is crucial for anticipating long-term ecosystem resilience and nature's contributions to people (Bjorkman et al., 2018; Cardinale et al., 2012).

Previous studies exploring relationships between biodiversity and the environment predominantly relied on taxonomic methods to assess the impact of biodiversity on ecosystem functioning (Meyer and Kröncke, 2019). In contrast to taxonomic methods, trait-based approaches focus on functional traits, i.e., traits that represent their morphological, physiological, biochemical or phenological characteristics. These traits are thought to be highly relevant to plant responses to the environmental stress and their impact on wider ecosystem properties (Díaz et al., 2013). By analysing functional traits, we can better understand how plants adjust or adapt to different environmental conditions (Kergunteuil et al., 2019), explain productivity in forests (Zhang-Zheng et al., 2024a, Zhang-Zheng et al., 2024b), and shed light on the role of plants in ecosystem processes (Díaz et al., 2013). Two metrics are widely used to quantify functional trait composition: the community-weighted mean (CWM) and community-weighted variance (CWV). CWM and CWV correspond to the average and variance in trait values within a community, weighted by the relative abundance (Laliberté and Legendre, 2010) or basal area (Aguirre-Gutiérrez et al., 2025; Pla et al., 2012) of each species. CWM represents the dominant trait values within a community and reflects the average functional characteristics shaped by the most abundant species, while CWV measures the trait diversity within the community and indicates the range and variability of functional strategies present.

Functional diversity is a vital component of biodiversity that captures the range and distribution of plant functional traits across spatial scales (Díaz et al., 2013; Ma et al., 2019). It is a determinant of ecosystem processes (Hooper et al., 2005), ecosystem resilience to environmental change (Aguirre-Gutiérrez et al., 2025; Folke et al., 2004), and provision of nature's benefits to people (Díaz et al., 2007; Laliberté and Legendre, 2010). As a commonly used functional diversity metric, functional dispersion quantifies the extent of trait dissimilarity within plant communities (Cadotte et al., 2013), elucidating how divergent or convergent species are in a community in terms of their functional traits. It is expected that higher functional dispersion (i.e., variation in plant trait values in the community) would render higher resilience to environmental change as at least some species should be able to thrive under the changing conditions (Hooper et al., 2005).

In addition, functional redundancy is the degree to which multiple species within an ecosystem show similar functional attributes and therefore are assumed to perform similar ecological roles or functions. This potentially suggests that when one species disappears, other species with similar trait values would be able to carry out the same ecosystem functions than the species lost (Rosenfeld, 2002). Ecosystems with low functional redundancy may be more vulnerable to environmental changes because there are fewer functionally similar species able to fill the roles of the species that are lost (Rosenfeld, 2002). Hence, functional redundancy is thought to be important for ecosystem stability and resilience in the face of disturbances, including extreme climatic events (Oliver et al., 2015). Therefore, assessing both functional diversity and redundancy in an ecosystem is particularly relevant for understanding forest resilience to environmental change (Carmona et al., 2016; Schneider et al., 2017).

Trait-based approaches have been valuable in describing and predicting ecosystem functions at the individual-to-plot scales. However, their upscaling to whole ecosystems and beyond has proven challenging (Suding et al., 2008). Still, recent advances in remote sensing techniques have allowed upscaling of some functional traits to global scales and the assessment of functional diversity continuously in space for relatively small areas (Hauser et al., 2021; Helfenstein et al., 2022; Schneider et al., 2017). Remote sensing platforms, including light detection and ranging (LiDAR), multispectral, and image spectroscopy data from both drone and satellite sensors, enable continuous and repeatable data acquisition that can be used to model and map functional traits across ecosystems (Aguirre-Gutiérrez et al., 2025; Wang and Gamon, 2019). Specifically, high-resolution LiDAR and spectral (including multispectral and image spectroscopy) data acquired from drone platforms can be used to characterise forest structural attributes (e.g., canopy height) and canopy reflectance properties, respectively, both of which are closely linked to functional traits (Asner et al., 2017; Camarretta et al., 2020; Kamoske et al., 2021). These detailed measurements at local scales offer critical insights into trait-environment relationships but are often spatially constrained. By integrating such plot-scale observations with coarser-resolution satellite-based remote sensing data, it becomes possible to bridge the spatial "scale-gap" (Thomson et al., 2021) to extend trait-based ecological information from individual plots to entire landscapes or regions (Jetz et al., 2016; Thomson et al., 2021; Wang and Gamon, 2019). The multiscale integration of remote sensing and trait-based ecology represents a scalable and essential approach for understanding functional biodiversity across complex landscapes, particularly in data-poor regions such as the temperate forests of South America (Kier et al., 2005; Sheffield et al., 2018).

Despite the capabilities of remote sensing approaches to upscale and predict some functional attributes, there is a lack of understanding about mapping and predicting variability in plant functional traits distribution (Butler et al., 2017) and plant functional diversity and redundancy at large spatial scales (Hortal et al., 2015), particularly in temperate forests beyond North America and Western Europe (Echeverría-Londoño et al., 2018). Besides remotely sensed imagery, environmental variables are also crucial for mapping plant functional traits and inferring functional diversity and redundancy as they shape the conditions under which plants grow and interact (Fortunel et al., 2014; Krishnadas et al., 2018; Wieczynski et al., 2019). Variation in climate, soil properties, topography, and hydrological stress directly influence the expression and performance of plant functional traits. These traits, in turn, determine how plants interact with each other and their environment, affecting overall community structure and ecosystem processes (Díaz et al., 2013; Zirbel et al., 2017). Variation in these biotic and abiotic drivers underpin the adaptation capacity of plants, and it could be expected that higher variation in ecological niches would also lead to a wide array of vegetation functional trait adaptation.

Here, we combined leaf and stem trait data measured *in-situ* from 8104 individual trees across 16 permanent forest plots in Chile with multi-scale remotely sensed data from multiple platforms and diverse environmental variables to model and predict community-level plant functional composition across a large latitudinal and environmental gradient using the Random forests algorithm. Trait data included leaf and stem morphological traits, leaf nutrients, hydraulic, and photosynthetic traits. The plots were distributed across a large latitudinal gradient extending from Mediterranean climate at $\sim$ 30°S to cold temperate climate at $\sim$ 53°S, covering a large annual rainfall (450–4500 mm) and mean annual temperature gradient (5.7–13 °C). Our main objectives were to 1) test if and to what extent functional trait composition, diversity, and redundancy can be inferred using remotely sensed data; 2) evaluate how community-level tree functional trait composition, diversity, and redundancy vary across the latitudinal and environmental gradients using both field-based data and spatially explicit model predictions; and 3) identify and quantify the main

environmental drivers of distributions of functional trait composition, diversity, and redundancy. We expect higher tree trait variation and higher functional diversity and lower redundancy in areas with more varied climate, topography and soil conditions. Conversely, we expect lower trait variation and higher functional redundancy in areas where climates are more restrictive, or more extreme for plant growth, such as in very cold or very warm areas often impacted by drought.

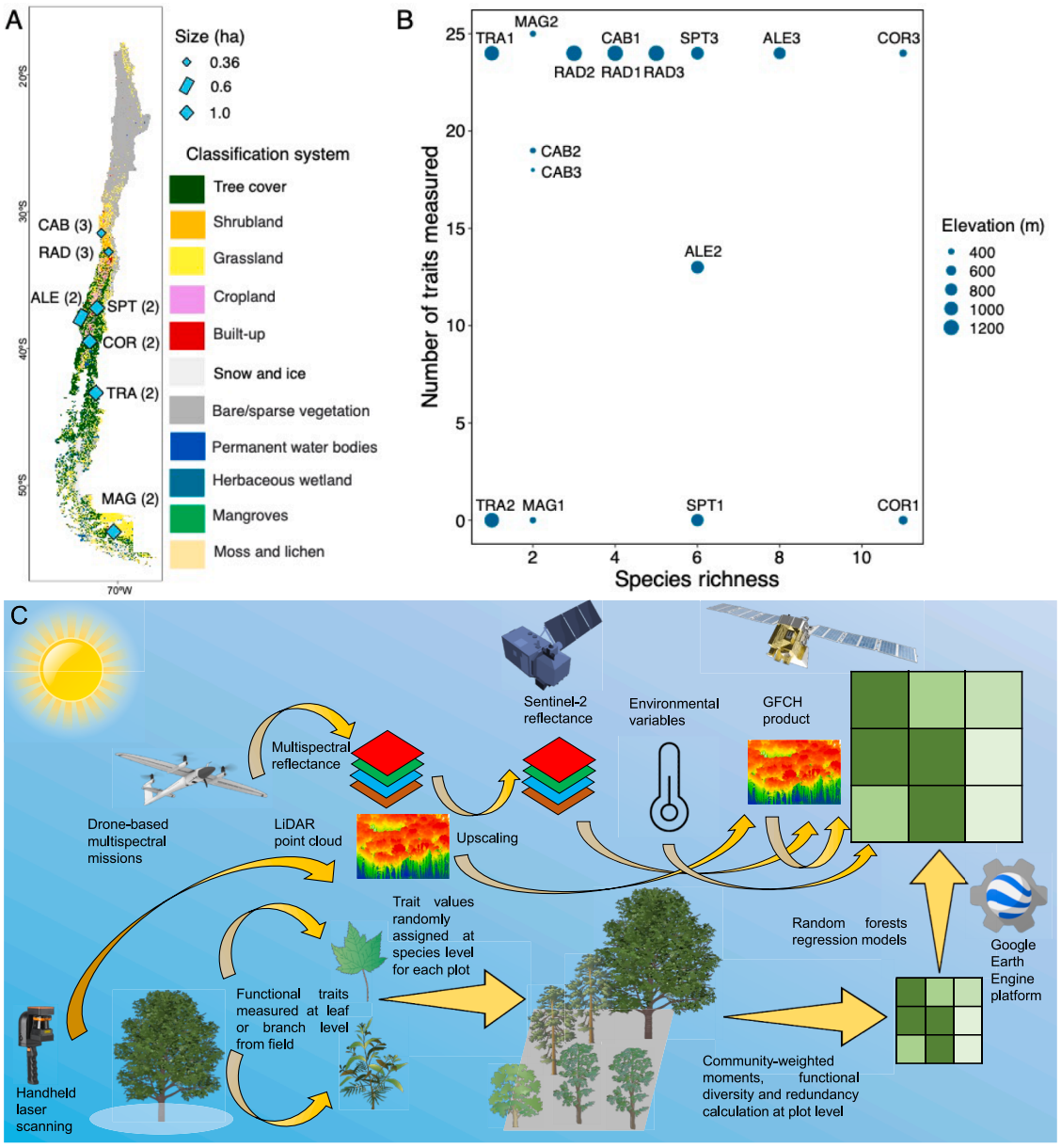

Fig. 1. Schematic of the process followed to model and map plant functional trait composition, diversity, and redundancy across forests in the study area. (**A**) Geographic locations of seven sites across a large latitudinal gradient. Site locations are shown by cyan rectangles with black boundaries. The number in brackets after the abbreviated site name corresponds to the number of plots in that site. Plot sizes within each site are shown by the size of the cyan rectangle (0.36 ha, 0.6 ha, or 1.0 ha plots). Note that all the rectangles are magnified for visualisation purposes. The background map is based on the WorldCover v200 land use and land cover product. (**B**) Detailed information on species richness and the number of traits measured in the field for each plot. The size of each dot indicates the elevation of the plot. Note: there is no trait measurement in plots COR1, MAG1, SPT1, and TRA2, but the species identified in these plots also exist in other plots. (**C**) Mapping plant functional trait composition, diversity, and redundancy with remote sensing and trait-based methods. This process integrates field-collected trait data with advanced remote sensing technologies. In the field, we collected leaf and stem samples from individual trees, and these samples were subsequently analysed in the lab to measure and calculate plant functional traits (see Supplementary: Sampling design and Trait measurements). We also obtained drone-level multispectral images and handheld LiDAR data for most forest plots. For plots without drone multispectral images (SPT1, ALE2, COR1, COR3, and MAG1) or handheld LiDAR data (COR1 and COR3), Planet SuperDove multispectral images and the global forest canopy height (GFCH) product were used. Trait community-weighted means and variances were calculated, representing trait averages and variability, and functional diversity and redundancy were derived from these traits at plot level. We used Random forests regression to establish the link between multispectral, LiDAR, environmental variables and functional traits. To extend these insights from plot to landscape level, we utilised satellite-based remotely sensed data, including Sentinel-2 (multispectral reflectance), the GFCH product (LiDAR-derived canopy height), environmental variables including TerraClimate (climatic variables), SoilGrids (soil properties), SRTM (topography), and ECOSTRESS (hydrological stress). (For interpretation of the references to colour in this figure legend, the reader is referred to the web version of this article.)

2. Methods and materials

2.1. Study area

The study area spans the temperate forests of Chile, South America, which covers a broad latitudinal gradient from approximately 30°S to 53°S. This range encompasses diverse forest ecosystems, including Mediterranean forests (~30°S to ~ 35°S) (Cueto et al., 2025), Valdivian rainforests (~35°S to ~ 42°S) (NAHUELHUAL et al., 2007), Austral forests (~42°S to ~ 48°S) (Huertas Herrera et al., 2023), and Magellanic subpolar forests (~48°S to ~ 53°S) (Rozzi et al., 2023). The local climate varies considerably along this gradient, with a wide range of environmental conditions, including significant variation in annual precipitation (450–4500 mm) and mean annual temperature (5.7–13 °C). In the northernmost Mediterranean zone, the climate is characterised by hot, dry summers and mild, wet winters (Kaiser et al., 2008). Between 35°S and 42°S, the climate transitions to a temperate rainforest type, typical of the Valdivian rainforests, where consistent high annual rainfall (often exceeding 3000 mm) and cooler temperatures create a humid environment (Tecklin et al., 2011). Further south, from 42°S to 53°S, the climate shifts to colder, wetter conditions in the Austral forests and Magellanic subpolar forests, which experience frequent rainfall and cold spells (Le Roux, 2012; Rozzi et al., 2023).

2.2. Field measurements

We conducted vegetation censuses of 8104 individuals (identified to species level) with diameter at breast height $\geq$ 10 cm across 16 vegetation plots in seven sites along a wide latitudinal and elevational gradient (from 327.34 to 1251.71 m). Specifically, there are three 0.36-ha plots in Las Cabras (CAB), three 0.36-ha plots in Radal Siete Tazas (RAD), two 1-ha plots in San Pablo de Tregua (SPT), two 0.6-ha plots in Alerce Costero National Park (ALE), two 1-ha plots in Correntoso (COR), two 1-ha plots in Trapananda National Reserve (TRA), and two 1-ha plots in Magallanes National Reserve (MAG) (Fig. 1A, B and Tables S1 and S2). These plots largely represent temperate forests, but the CAB plots are also representative of drier and shrubby vegetation. Here, for simplicity we refer to all of them as "forests". The field data collection was carried out between 10 February 2020 and 25 January 2022. To get a holistic view of community dynamics and acquire a comprehensive assessment of functional diversity and redundancy within temperate forests, we measured and calculated a diverse set of leaf and stem functional traits spanning four functional categories (Tables S3 and S6). These included: eight morphological traits: leaf fresh weight (FW, g), leaf dry weight (DW, g), leaf area (LA, cm^2), specific leaf area (SLA, $cm^2 \cdot g^{-1}$), leaf mass per area (LMA, $g \cdot cm^{-2}$), leaf dry matter content (LDMC, $mg \cdot g^{-1}$), trunk wood density (TWD, $g \cdot cm^{-3}$), and branch wood density (BWD, $g \cdot cm^{-3}$). SLA and LMA were derived from directly measured traits (i.e., LA and FW), although SLA and LMA are mathematically inverses, they offer different insights. SLA is commonly used in growth analyses due to its positive linear relationship with relative growth rate, whereas LMA is more intuitive when analysing structural investment in leaves (Poorter et al., 2009). Six nutrients (i.e., leaf chemical traits): calcium (Ca, %), potassium (K, %), magnesium (Mg, %), nitrogen (N, %), and phosphorus (P, %) content in leaves, and the ratio of leaf nitrogen content and leaf phosphorus content (N/P, unitless). Five hydraulic traits: water potential at which 50 % and 88 % of hydraulic conductivity is lost (P50 and P88, MPa), minimum water potential (WPmd, MPa), and safety margin for P50 and P88 (SM50 and SM88, MPa). Five photosynthetic traits: temperature at the carbon compensation point (TmaxL, °C), temperature of optimum photosynthesis (Topt, °C), photosynthetic rate at optimum temperature (Aopt, $\mu mol \cdot CO_2 \cdot m^{-2} \cdot s^{-1}$), breadth of the temperature optimum (TspanL, °C), and temperature at which the maximum quantum yield of the photosystem II declines to 50 % (T50, °C). Together, these traits offer insights into different aspects of plant function: physical structure, nutrient cycling and ecosystem productivity, water transport strategies, and the efficiency of energy capture and utilisation. Plant traits were collected for the most abundant species, so that we have a coverage of at least 80 % of the plot's basal area with trait values.

2.3. Plot level remote sensing: Multispectral images and laser scanning

We implemented drone missions to obtain high-resolution multispectral images (~5 cm pixel) using the MicaSense Altum multispectral camera across 11 plots. We also collected handheld LiDAR data using the ZEB1 3D handheld laser scanner from GeoSLAM across 14 plots. For the plots without drone multispectral or handheld LiDAR data due to environmental constraints, we obtained analysis-ready SuperDove multispectral (3 m, containing either five or eight bands, see Table S7) satellite images from PlanetLabs (https://www.planet.com/) and also extracted canopy height information from the global forest canopy height (GFCH) product (Potapov et al., 2021) (Table S8).

We processed the six-band MicaSense Altum-PT multispectral images using the Pix4Dmapper software (https://www.pix4d.com/product/pix4dmapper-photogrammetry-software/), following the workflow outlined in the MicaSense Pix4D processing guide (https://support.micasense.com/hc/en-us/articles/115000831714-How-to-Process-MicaSense-Sensor-Data-in-Pix4D). The main steps included image radiometric correction and calibration (no correction for the long-wave infrared (LWIR) band because the thermal imager in Altum was already radiometrically calibrated) using reflectance panel and sunshine sensor data, and generation of reflectance maps for each spectral band. We then merged the reflectance maps into one multi-layer virtual raster (.vrt file) using the gdalbuildvrt programme of the Geospatial Data Abstraction Library (Rouault et al., 2024) in the command line for each plot. Finally, we loaded the.vrt file into the QGIS software and exported it as a raster (.tif file) for each plot. Note that we kept the blue, green, red, red edge, and near-infrared (NIR) bands due to their consistent presence in both drone images and SuperDove satellite images. Additionally, we calculated four vegetation indices, the normalised difference vegetation index (NDVI) (Myneni et al., 1995), normalised difference red edge index (NDRE) (Gitelson and Merzlyak, 1994), soil-adjusted vegetation index (SAVI) (Huete, 1988), and modified soil-adjusted vegetation index (MSAVI) (Qi et al., 1994) to model the functional trait composition, diversity, and redundancy (Table S9). These indices were selected because they are sensitive to vegetation structure, canopy greenness, and photosynthetic activity, which are closely related to plant functional traits. NDVI and NDRE are widely used indicators of chlorophyll content and photosynthetic potential, making them relevant for modelling traits linked to productivity and leaf function (Aguirre-Gutiérrez et al., 2025; Helfenstein et al., 2022; Sun et al., 2024). SAVI and MSAVI adjust for soil background effects and are especially useful in areas with varying vegetation cover, which helps to better capture spatial heterogeneity relevant to functional trait distributions and biodiversity metrics (Aguirre-Gutiérrez et al., 2025; Hussain et al., 2020; Sun et al., 2024; Wang et al., 2016). For the LiDAR data, we generated canopy height from the LiDAR point cloud using the LAStools processing software (https://rapidlasso.de/) or directly from the GFCH product. When using LAStools, we first removed outliers with the LASview tool. Ground points were classified with the LASground_new tool using hyperfine search criteria to accurately identify ground points. We then extracted canopy height for all returns above a 2-m threshold with the LASheight tool following default settings, thus separating canopy from understory vegetation, and we removed duplicate returns with the LASduplicate tool.

2.4. Environmental variables

We obtained variables related to climate, soil properties, topography, and hydrological stress. For climatic data, we collected three long-term monthly climatic variables and calculated their mean values

(1983 to 2022), namely temperature, vapour pressure deficit (VPD), and climatological water deficit (CWD), using the TerraClimate dataset (Abatzoglou et al., 2018) at a spatial resolution of ~ 4 km (https://www.climatologylab.org/terraclimate.html). Furthermore, we calculated the maximum climatological water deficit (MCWD), which is defined as the most negative value of CWD, to describe the accumulated water stress that occurs across a dry season (Malhi et al., 2009):

$$CWD_{(n)} = CWD_{(n-1)} + P_{(n)} - E_{(n)} \quad (1)$$

$$Max(CWD_{(n)}) = 0 \quad (2)$$

$$CWD_{(0)} = CWD_{(12)} \quad (3)$$

$$MCWD = Min(CWD_{(0)}, CWD_{(1)}, ..., CWD_{(12)}) \quad (4)$$

where n ($n = 1, 2, \ldots, 12$) is the index of a month over a calendar year, and P and E are precipitation (mm/month) and evapotranspiration (mm/month). We set $CWD_{(6)} = 0$ as June is normally the wettest month in Chile (Araya-Osses et al., 2020) and therefore assume the soil is saturated and applied this calculation to the mean annual cycle of precipitation (Malhi et al., 2009). We also calculated the additive inverse of MCWD whereby positive MCWD values are an intuitive indication of increases in water stress.

We gathered soil data from the SoilGrids database (https://soilgrids.org/) at a spatial resolution of 250 m (Hengl et al., 2017). All soil variables were extracted for the top 30 cm layer and averaged across depth intervals (0–5 cm, 5–15 cm, and 15–30 cm) using depth-weighted means (Quick and Chadwick, 2011). The following five variables were summarised at the plot level: cation exchange capacity at pH 7 (CEC, in mmol(c)/kg), pH in water (pHH_2O, pH × 10), soil organic carbon (SOC, in dg/kg), clay and sand content (both in g/kg). These variables capture key aspects of soil fertility and structure. Specifically, CEC reflects the soil's ability to retain and exchange nutrients, directly influencing plant nutrient availability. pHH_2O reveals soil acidity or alkalinity, which affects nutrient solubility and species tolerance. SOC represents the amount of organic matter, often linked to soil health and stress conditions. Finally, soil texture (clay and sand content) affects water-holding capacity, drainage, and root penetration, which are critical for plant growth and habitat suitability.

For topographic data, we obtained the digital elevation model from the shuttle radar topography mission (Farr et al., 2007) at 30 m (https://cmr.earthdata.nasa.gov/search/concepts/C1000000240-LPDAAC_ECS.html) and derived slope and aspect.

Lastly, using the ECOsystem Spaceborne Thermal Radiometer Experiment on Space Station (ECOSTRESS) (Fisher et al., 2020) we extracted evapotranspiration (ET), evaporative stress index (ESI), and water use efficiency (WUE) as indicators of hydrological stress. Specifically, we accessed 4383, 3917, and 4095 tiles for ET, ESI, and WUE, respectively, through AppEEARS at ~ 70 m spatial resolution (https://appeears.earthdatacloud.nasa.gov/) from 01 November 2019 to 31 January 2023.

2.5. Predicting community level traits and functional diversity and redundancy with satellite remote sensing

We used Sentinel-2 multispectral data (10 m) from the European Space Agency (Drusch et al., 2012) and the GFCH product (30 m) for predicting functional trait composition, diversity, and redundancy across forest areas in Chile. The Sentinel-2 mission comprises a constellation of two identical satellites, Sentinel-2A and Sentinel-2B, operating synergistically to capture imagery of the Earth's surface. These satellites are equipped with a multispectral instrument, capturing data across 13 spectral bands, ranging from visible to infrared wavelengths. This extensive spectral coverage allows for detailed analysis of vegetation health and land cover changes, making Sentinel-2 images invaluable for applications in ecology, forestry, and climate studies.

Specifically, we used the COPERNICUS/S2_SR_HARMONIZED collection available through Google Earth Engine (https://earthengine.google.com/) cloud computing platform (Gorelick et al., 2017), which provides atmospherically corrected and harmonised Level-2A surface reflectance data. As part of additional pre-processing, we masked cloud and cirrus pixels using the QA60 band (bits 10 and 11), and rescaled reflectance values to a 0–1 range by dividing by 10000. A median composite was generated from cloud-free images between 10 February 2020 and 25 January 2022 and clipped to the study area for analysis.

2.6. Identification of trait-trait correlations

We tested correlations between all functional traits (Fig. S1) and proposed the mean absolute within-category correlation index (MACI) that is defined as follows to identify key functional traits:

$$MACI = \frac{\sum_{m=1}^{M}\sum_{n=1}^{M}|C_{m,n}|}{M} \quad (5)$$

where M is the total number of different functional traits in the same category (i.e., morphological, nutrient, hydraulic, and photosynthetic traits), and in an $M \times M$ correlation matrix, m and n indicate the ordinal numbers of traits, where $C_{m,n}$ stands for the correlation value between the mth and the nth functional traits within the same trait category.

By setting the threshold as 0.9, functional traits whose MACI values were greater than 0.9 were excluded as they were highly correlated with other traits in the same category. We selected: 1) morphological (Mor) traits: FW, DW, LA, SLA, and TWD; 2) leaf nutrients (Nutr): N, P, Ca, and Mg content in leaves; 3) hydraulic (Hydr) traits: P50, P88, and WPmd, and 4) photosynthetic (Pho) traits: TmaxL, Topt, TspanL, and T50.

2.7. Calculating functional trait composition

We calculated the community weighted mean (CWM) and variance (CWV) of every functional trait using the individual's basal area as the weighting factor. Specifically, CWM and CWV are defined as follows:

$$CWM = \frac{\sum_{i=1}^{N} BA_i \times t_i}{\sum_{i=1}^{N} BA_i} \quad (6)$$

$$CWV = \frac{\sum_{i=1}^{N} BA_i \times (t_i - CWM)^2}{\sum_{i=1}^{N} BA_i} \quad (7)$$

where N is the total number of tree individuals in a community (i.e., a single plot), and BA_i and t_i denote the basal area and trait value of the ith individual, respectively.

2.8. Calculating functional diversity and redundancy

We calculated functional dispersion as a measure of functional diversity. Functional dispersion (FDis) (Laliberté and Legendre, 2010) is defined as the mean distance in multidimensional trait space of individual species to the centroid of all species. FDis quantifies the effective number of functionally distinct species for a given level of species dispersion and measures the spread and variability of species within the trait space. We calculated FDis across the four functional trait categories (morphology, nutrients, hydraulics, and photosynthesis) using the "dbFD" function of the R "FD" package (Laliberté et al., 2014):

$$FDis = \frac{\sum_{i=1}^{N} BA_i \times z_i}{\sum_{i=1}^{N} BA_i} \quad (8)$$

where BA_i is the basal area of species i in a plot, and z_i stands for the distance of species i in a plot to the weighted centroid of the N individual species in the trait space.

In addition, functional redundancy (FRed) measures the extent to

which species within a community share similar functional roles and helps infer the resilience and stability of ecosystems by indicating whether there are backup species that can compensate for the loss of others in terms of functional roles (Ricotta et al., 2016). To calculate FRed across the four functional trait categories, we employed the "uniqueness" function of the R "adiv" package (Pavoine, 2020). Specifically, in a community composed of *N* species:

$$FUni = \frac{\sum_{i=1}^{N} p_i \times \sum_{j=1}^{N} p_j \delta_{ij}}{\sum_{j=1}^{N} p_j (1 - p_i)} \quad (9)$$

$$FRed = 1 - FUni \quad (10)$$

where FUni is functional uniqueness that refers to the distinctiveness of species with similar traits measured at community level. p_i (where $0 < p_i \leq 1$ and $\sum_{i=1}^{N} p_i = 1$) represents the relative abundance of species *i*, and δ_{ij} denotes the pairwise functional dissimilarity between species *i* and *j*, where $\delta_{ij} = \delta_{ji}$ and $\delta_{ii} = 0$.

2.9. Predicting functional trait composition, diversity, and redundancy at plot level

We modelled CWM, CWV, functional diversity, and redundancy as a function of climate, soil, topography and the remote sensing data described above. For all remote sensing predictors, we calculated their mean and variance at the plot level. The data were then divided into seven categories: 1) spectral bands: blue, green, red, NIR, and red edge, 2) vegetation indices: NDVI, NDRE, SAVI, and MSAVI, 3) LiDAR, 4) climate: temperature, VPD, and MCWD, 5) hydrological stress: ET, ESI, and WUE, 6) topography: slope and aspect, and 7) soil: CEC, clay, sand, pHH_2O, and SOC. To simplify the model and avoid overfitting, we also tested the correlation between all variable's mean values (Fig. S2) and applied the MACI to each of them, dropping those whose MACI values were greater than 0.9. Eventually, mean and variance values of red, red edge, NIR, NDVI, NDRE, SAVI, MSAVI, height, MCWD, temperature, ET, ESI, WUE, slope, aspect, CEC, clay, sand, pHH_2O, and SOC were selected.

We then used machine learning (Random forests regression (Breiman, 2001)) to model the CWM, CWV, functional diversity and redundancy as a function of the above-mentioned variables. To optimise the two key parameters of the Random forests regression, namely the number of trees and the number of variables randomly selected at each split, we tested different combinations. The number of trees ranged from 5 to 100 with a step of 5, and the number of variables ranged from 1 (the minimum number of input bands) to 20 (the maximum number of input bands). To evaluate model performance, we split the dataset into 70 % for training and the remaining 30 % for testing. We then calculated the mean absolute error (MAE), root mean square error (RMSE), and coefficient of determination (R^2) to comprehensively evaluate the performance of all models. We also evaluated our models based on a leave-one-out cross-validation approach using the "caret" package in R (Kuhn, 2008). The optimal model is determined as the one with minimum RMSE value.

2.10. Key drivers of functional trait composition, diversity, and redundancy

To uncover key drivers of functional trait composition, diversity, and redundancy, we tested the importance of each input variable (VarImp) from the models created above. VarImp was calculated using the decrease in node impurities (i.e., the mean reduction in residual sum of squares), as implemented in the varImp function of the R "caret" package (Kuhn, 2008). We also calculated mean VarImp scores of each of the seven groups of input data to explore how different variables contribute to mapping functional traits and assessing FDis and FRed, after normalising the individual variable importance scores to express their relative contribution.

2.11. Scaling up from plots to the full study area

We identified forest sites across the study area by generating a forest mask using the "tree cover" class from the 10-m WorldCover v200 land use and land cover product (https://worldcover2021.esa.int/) (Zanaga et al., 2022). Then, we collated Sentinel-2 multispectral images from 2019 to 2023 and conducted pre-processing and applied all the optimal parameters gained from above to the Random forests regression via the Google Earth Engine (https://earthengine.google.com/) cloud computing platform (Gorelick et al., 2017) to predict functional trait composition, diversity, and redundancy (Fig. 1C).

3. Results

3.1. Spatial distribution of functional trait composition, diversity, and redundancy

We obtained spatial predictions of the trait community weighted mean (CWM) and variance (CWV) for each functional trait (Fig. 2, all trait maps see Figs. S3 to S10), as well as functional diversity (FDis) and redundancy (FRed) across the study area within forested regions. A bivariate map showing the joint distribution of FDis and FRed was presented in Fig. 3 (separate maps were provided in Figs. S11 and S12). Our models for CWM had an average $R^2 = 0.61$, while for CWV they had an average R^2 of 0.44 (Tables S10 to S13). The average R^2 for assessing the FDis and FRed were 0.48 and 0.52, respectively (Table S14).

For functional traits, there is a noticeable pattern in the latitudinal distribution between approximately 35°S and 42°S, where CWM and CWV values for almost all functional traits are relatively low compared to neighbouring regions. We also found distinct spatial distribution patterns of FDis and FRed across the gradient explored. Notably, we observed a latitudinal gradient wherein both FDis and FRed are high within a narrow band, primarily between latitudes 35°S and 42°S. Within this range, FDis exhibits a range from 0.86 to 2.06 with a mean value of 1.13 (mean values of 1.22, 1.21, 0.83, and 1.27 for $FDis_{Mor}$, $FDis_{Nutr}$, $FDis_{Hydr}$, and $FDis_{Pho}$, respectively, Fig. S11). Similarly, FRed ranges from 0.31 to 0.63 with a mean of 0.46 (mean values of 0.44, 0.46, 0.48, and 0.46 for $FRed_{Mor}$, $FRed_{Nutr}$, $FRed_{Hydr}$, and $FRed_{Pho}$, respectively, Fig. S12). There is a divergence in the dominance of the different metrics. Specifically, FDis is higher, with the mean value peaking at 1.29 (mean values of 1.53, 1.13, 1.30, and 1.21 for $FDis_{Mor}$, $FDis_{Nutr}$, $FDis_{Hydr}$, and $FDis_{Pho}$, respectively, Fig. S11) between latitudes 30°S and 35°S. In contrast, within the latitudinal range of 42°S to 48°S, FRed dominates across the four trait groups with the mean value reaching 0.54 (mean values of 0.56, 0.52, 0.54, and 0.52 for $FRed_{Mor}$, $FRed_{Nutr}$, $FRed_{Hydr}$, and $FRed_{Pho}$, respectively, Fig. S12). Finally, both FDis and FRed are low between 48°S to 53°S, with mean FDis being 0.71 (mean values of 0.65, 0.81, 0.66, and 0.71 for $FDis_{Mor}$, $FDis_{Nutr}$, $FDis_{Hydr}$, and $FDis_{Pho}$, respectively, Fig. S11) and mean FRed being 0.23 (mean values of 0.24, 0.23, 0.20, and 0.24 for $FRed_{Mor}$, $FRed_{Nutr}$, $FRed_{Hydr}$, and $FRed_{Pho}$, respectively, Fig. S12).

3.2. Drivers of functional trait composition, diversity, and redundancy across the latitudinal gradient

Based on variable importance (VarImp) analysis for CWM (Fig. 4 and Figs. S13 to S16), the top-ranking variable for predicting CWM_{Mor} and CWM_{Nutr} is hydrological stress (mean VarImp = 31.99 for CWM_{Mor} and mean VarImp = 36.22 for CWM_{Nutr}), while soil properties contribute the most in predicting CWM_{Hydr} (mean VarImp = 23.32) and CWM_{Pho} (mean VarImp = 36). Climate follows closely after hydrological stress and soil properties for predicting CWM_{Nutr} (mean VarImp = 21.74) and CWM_{Hydr} (mean VarImp = 19.20). For CWV (Fig. 4 and Figs. S13 to S16), soil properties are identified as the most important variable in the

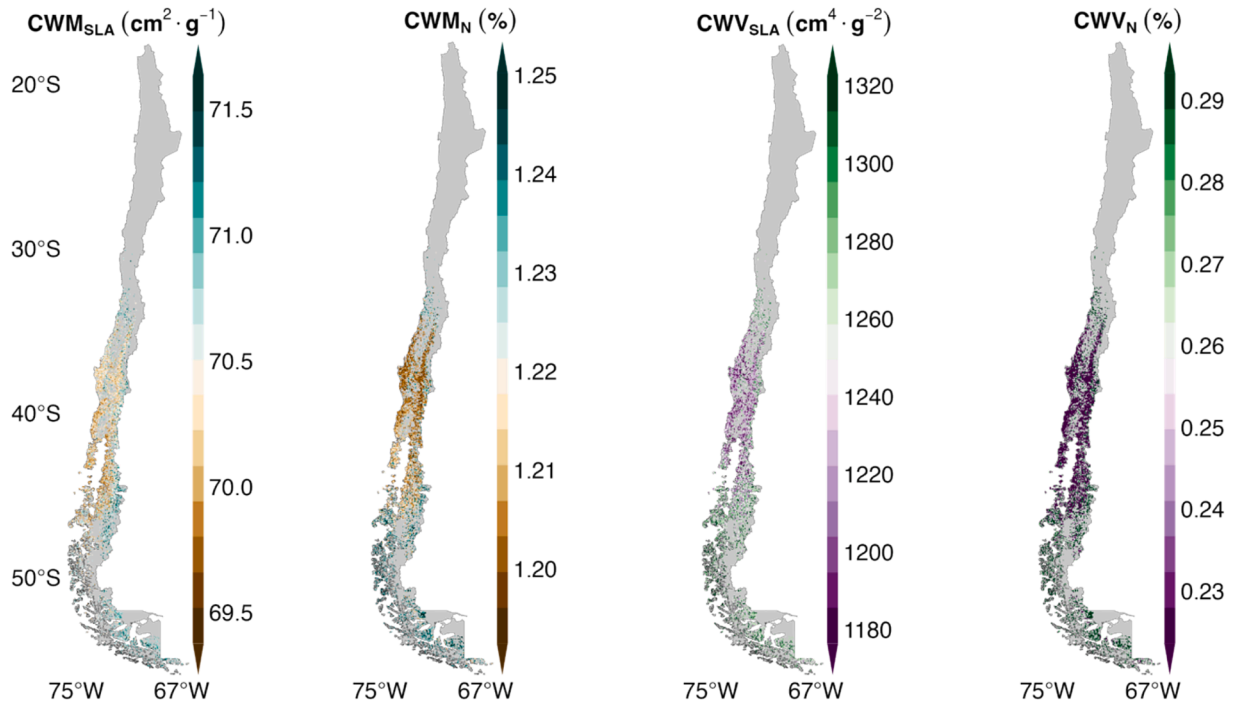

Fig. 2. Geographic distribution (CWM) and variation (CWV) maps of SLA and leaf nitrogen (N) content. Distribution and variation maps of all traits are included in Figs. S3 to S10.

case of morphology, nutrients, and hydraulics (mean VarImp = 41.60, 24.97, and 33.99 for CWV_{Mor}, CWV_{Nutr}, and CWV_{Hydr}, respectively). Notably, topography ranks first in predicting CWV_{Pho} (mean VarImp = 23.67), and it is also the second most important predictor for CWV_{Mor} (mean VarImp = 28.65) and CWV_{Nutr} (mean VarImp = 21.23).

Hydrological stress and soil properties emerge as the predominant drivers of FDis and FRed (Fig. 5) across all trait groups, with notable mean VarImp of 27.97 and 21.28 for FDis, and 28.13 and 22.88 for FRed, respectively. Moreover, hydrological stress is the only type of variable whose importance scores were consistently high for driving both FDis and FRed in all trait groups, while plant canopy height contributed little to predicting FRed of morphology, nutrients, and photosynthesis.

Soil properties (VarImp = 30.81 for FDis) and climate (VarImp = 36.27 for FRed) emerge as the primary drivers in terms of morphology. For leaf nutrients, the importance of hydrological stress (VarImp = 33.29 for FDis and VarImp = 48.76 for FRed) and soil properties (VarImp = 25.15 for FDis and VarImp = 21.58 for FRed) is prominent. When considering hydraulic traits, hydrological stress (VarImp = 43.60) and soil properties (VarImp = 33.75) are found as the most important drivers of FDis and FRed, respectively. Lastly, photosynthetic FDis and FRed are notably driven by hydrological stress (VarImp = 21.50 for FDis and VarImp = 27.84 for FRed) and soil properties (VarImp = 20.15 for FDis and VarImp = 26.87 for FRed). Additionally, climate also demonstrates high importance in driving FDis (VarImp = 17.32) and FRed (VarImp = 21.48) of photosynthesis as it ranks third closely to soil properties for both metrics.

4. Discussion

4.1. Inferring plant functional trait composition, diversity, and redundancy using remote sensing approaches

The integration of plot-level *in-situ* plant functional traits with remotely sensed data acquired across multiple spatial scales and platforms provided not only a comprehensive understanding of trait distributions and variances, but also holistic insights into functional diversity and redundancy (inferred by FDis and FRed in this study). Using multispectral drone imagery and handheld LiDAR scans acquired at the plot-level, we obtained detailed spectral and structural information of forest functional composition at fine scales. Then, we used the satellite data to upscale our results to the extent of the full study area. In doing so, we demonstrate the potential to scale up plot-level ecological understanding with high accuracy across large latitudinal and environmental extents.

The ability to scale up from plot-level data to large spatial extents with remote sensing allows us to generate maps that predict the spatial distribution and variation of plant functional trait composition, diversity, and redundancy across vast areas. By combining multispectral and LiDAR data with *in-situ* measurements, remote sensing proves to be a high-resolution and cost-effective means to monitor and predict the distribution and variability of trait composition, diversity, and redundancy with optimal predictive accuracies (Objective 1). These spatially explicit predictions further allowed us to evaluate how functional trait composition, diversity, and redundancy vary across broad latitudinal and environmental gradients (Objective 2), and to identify the most important environmental drivers shaping their distribution and variation across the landscape (Objective 3). Together, these outcomes highlight the potential of integrating field-based trait data and multi-source remote sensing to advance landscape-scale assessments of biodiversity and forest function. These predictions are crucial for assessing how climate change, extreme weather events, and other environmental stressors may affect forest resilience (Helfenstein et al., 2022), and are therefore not only vital for conservation and forest management strategies but also for developing responses to mitigate the impacts of environmental change.

4.2. Variation of plant functional traits across latitudinal and environmental gradients

The intermediate region of the study area includes the Mediterranean-Temperate transition zone (35.5°-39.5°S), as well as a rainy, temperate climate zone south of 40°S (up to 48°S), characterised by a temperate climate with dry summers and warm temperatures

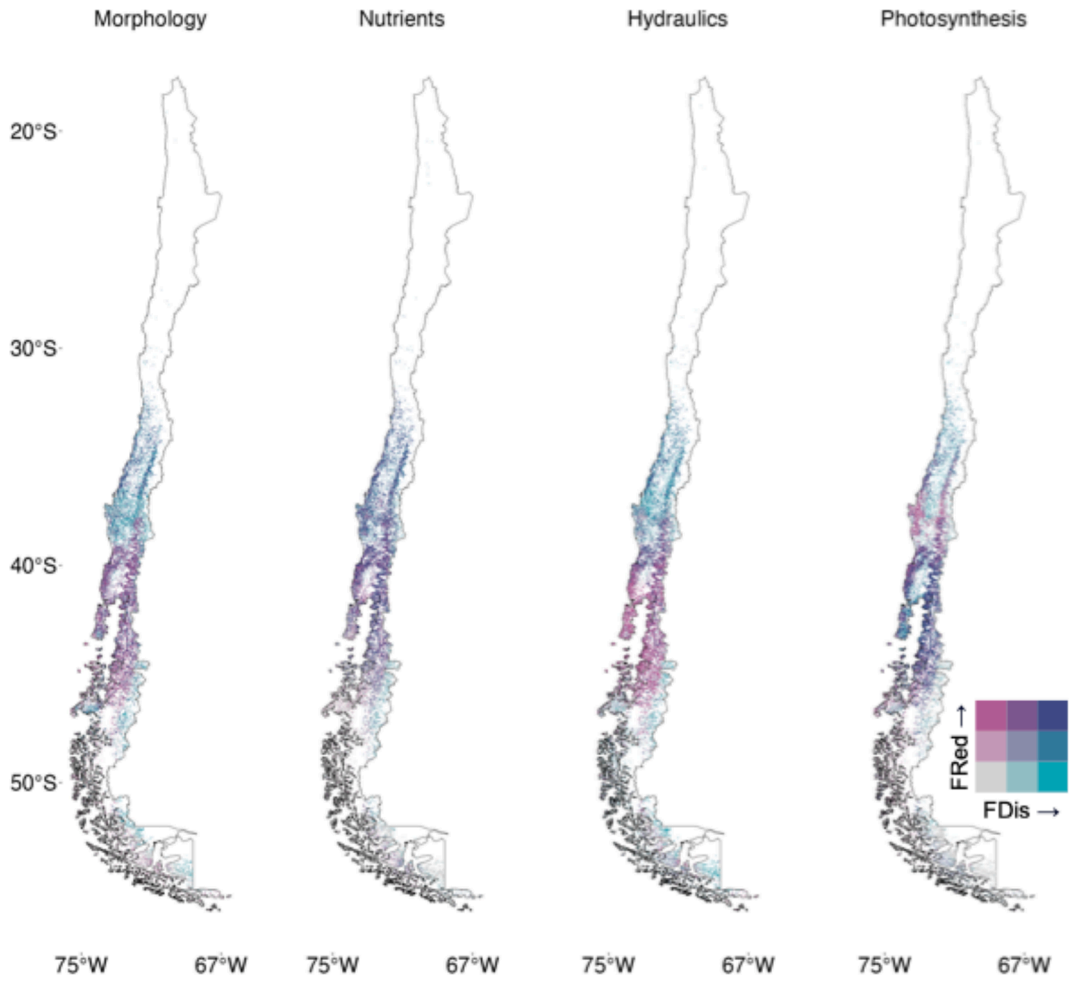

Fig. 3. Bivariate maps of FDis and FRed for morphologic, nutrient, hydraulic, and photosynthetic traits within Chilean temperate forest ecosystems. In the legend located in the bottom right, the horizontal axis represents the range of FDis values, while the vertical axis similarly represents the range of FRed values. The colour gradient shows the joint distribution of FDis and FRed, where grey indicates low values of both variables, turquoise indicates high FDis and low FRed, magenta represents high FRed and low FDis, and navy indicates high values of both variables. Individual maps of FDis and FRed are shown in Figs. S11 and S12. (For interpretation of the references to colour in this figure legend, the reader is referred to the web version of this article.)

(Sarricolea et al., 2017). Despite the overall favourable climatic conditions, including cold to moderate temperatures and sufficient moisture (Cavieres et al., 2007), the reduced trait variability within plant communities suggests a regime characterised by ecological homogenisation (Gámez-Virués et al., 2015). Forests in this area are characteristic of the temperate type with mostly evergreen species (Pérez et al., 2003). The dominance of species with similar functional traits in this area may be attributed to the convergence of environmental factors, such as soil properties (Grime, 2006) and topographic features (Schmitt et al., 2020), which limits the dominance of more diverse functional strategies among plant species. Furthermore, more moderate temperatures, compared to the north and south of this area, and the absence of a pronounced dry season, especially toward the south, may contribute to the stabilisation of plant communities (Isbell et al., 2015) and the reduction in trait variability (Dell et al., 2011) by minimising the influence of seasonal water availability on species composition and functional trait distributions.

In the central portion of the study area (spanning from approximately 30°S to 35°S), several functional traits, i.e., FW, DW, TWD, P50, and P88, consistently exhibited both high CWM and CWV values, likely driven by the Mediterranean climatic conditions of this region (Garreaud et al., 2020). Considering that this pattern mainly appears in morphological and hydraulic traits that are paramount for species survival and reproduction in Mediterranean climates with prolonged drought, high temperatures, and winter rainfall, high CWM indicates prevalent trait values optimised for these climatic conditions (Bruelheide et al., 2018). Small, thick leaves and deep root systems, which enhance water retention and uptake efficiency, are characteristic of this type of climate (Wasson et al., 2012). Concurrently, high trait variance suggests species' abilities to fine-tune these traits to specific microhabitats (Denelle et al., 2019) or respond to localised variations in resource availability (Candeias and Fraterrigo, 2020), contributing to the community's ecological diversity and resilience within the Mediterranean ecosystems.

Conversely, in the southern portion of the study area, the observed increase in both CWM and CWV values for most traits reflects a shift in ecological dynamics within a cold oceanic (temperate/subpolar) climate regime, spanning from approximately 42°S to 53°S. This higher trait variability suggests an ecological setting characterised by colder temperatures and maritime influences (Vilà-Cabrera et al., 2015). The dominance of traits with higher CWM values indicates a commonness of functional strategies adapted to the colder environmental conditions (Bjorkman et al., 2018) typical of this southernmost region. Traits related to temperature responses, such as TmaxL and Topt, exhibited notably higher CWM values, indicating the persistence of certain functional strategies adapted to the cooler temperatures (Laughlin et al., 2018). Additionally, the dominance of cold-adapted species and the presence of diverse ecological niches shaped by maritime influences

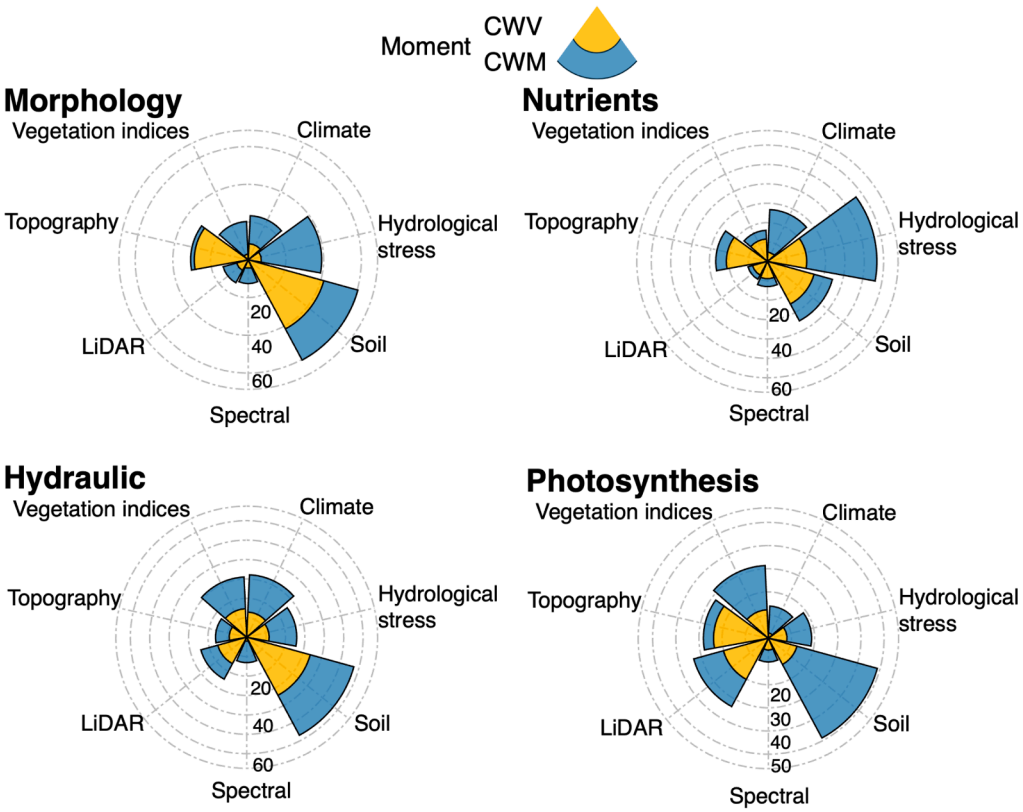

Fig. 4. Mean variable importance of input data groups for predicting community-weighted mean (CWM) and community-weighted variance (CWV) of the four categories of functional traits. In each of the polar stacked bar charts, the seven input data types were assigned to specific spokes, along which stacked bars were drawn. The height of each segment within the stacked bar corresponded to the importance of the variable it represented. Different colours were used to distinguish between CWM and CWV. Numbers alongside the grey radial axis denote scale values reflecting normalised importance scores, with the maximum scale adjusted to the highest observed group mean importance score.

contribute to the higher trait variability observed in the southern region.

4.3. Understanding plant functional diversity and redundancy across temperate forests

Functional diversity and redundancy complement each other in capturing different aspects of community structure and functioning. High diversity with low redundancy may indicate a community with diverse strategies, while low diversity coupled with high redundancy may suggest a more functionally homogeneous community (Mouchet et al., 2010).

As expected, we reveal a combination of both high FDis and FRed emerging from dense tree cover and high species diversity in the intermediate region of the study area, spanning between latitudes ~ 35°S and ~ 42°S. This region is a biodiversity hotspot (Echeverría et al., 2006; Myers et al., 2000), where favourable climatic conditions and varied habitats facilitate the coexistence of a diverse array of plant species with distinct functional traits (Kraft et al., 2015). In light of the transition from the Mediterranean climate in the north to the more temperate rainy climate in the south, the observed high FDis signifies the presence of a wide range of functional strategies among plant communities, while the concurrent high FRed suggests a robustness in ecosystem functioning and resilience to ongoing environmental changes and human disturbances (Oliver et al., 2015). This balance between FDis and FRed suggests a high-resilience system, well-adjusted to a mild climate with ample moisture (Correia et al., 2018). However, considering this region's status as a highly threatened area in which forests have experienced extensive conversion to exotic forest plantations (Braun et al., 2017; Miranda et al., 2017), the high FDis and FRed emphasises the importance of preserving ecological integrity. With reduced trait variability and increased environmental homogenization in this transitional zone, conservation efforts could target restoration, habitat connectivity enhancement, and community engagement to mitigate degradation.

The high FDis observed across ~ 30°S and ~ 35°S, characterised by Mediterranean climate with long dry and hot summers, demonstrates the remarkable adaptation of the regional flora to the harsh environmental conditions. The observed extensive variability in plant functional traits reflects the diverse strategies adopted by species to thrive in water-limited environments (Ruiz-Benito et al., 2017). Such adaptations likely contribute to the high taxonomic diversity observed in this region, as plant species have evolved specialised traits, i.e., SLA and P50 (Costa-Saura et al., 2016), to optimise resource acquisition and utilisation and constrain plant gas exchange under drought conditions (Vilagrosa et al., 2014). Our findings highlight the ecological significance of Mediterranean ecosystems as hotspots of biodiversity and contribute to the overall resilience of the continent's flora.

In addition, our findings carry implications for understanding ecological dynamics and biodiversity conservation across the continent. These implications are particularly relevant in light of recent environmental disturbances. For example, extreme fire weather, referring to a combination of high temperature, low humidity, and strong winds that promote the occurrence and intensity of wildfires, was observed in connection with climate change and El Niño in 2017 (De la Barrera et al., 2018) and 2023 (Bowman et al., 2019; Cordero et al., 2024). The region has also experienced climate-induced large-scale forest browning driven by the exceptionally severe megadrought since 2010 (Miranda et al., 2023). The identification of regions with high FDis highlights the critical role of functional diversity in shaping ecosystem resilience in the face of

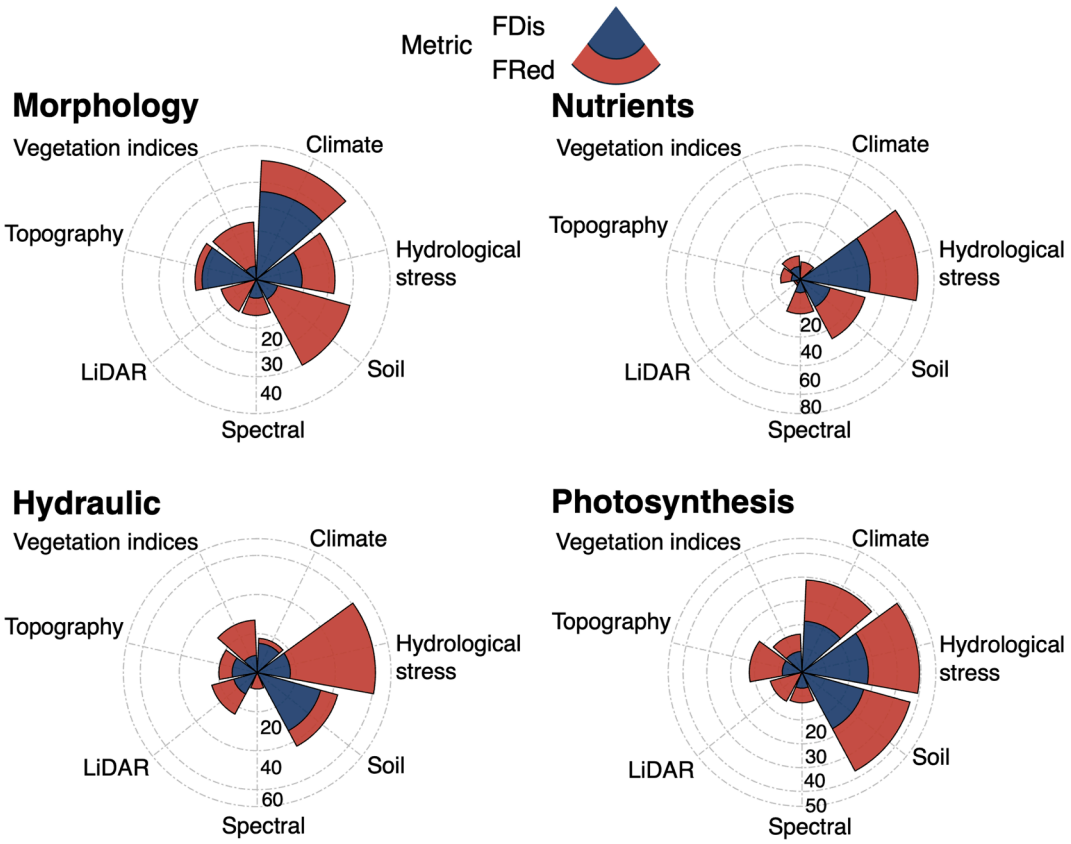

Fig. 5. Mean variable importance of input data groups for predicting functional diversity (FDis) and redundancy (FRed) of the four categories of functional traits. In each of the polar stacked bar charts, the seven input data types were assigned to specific spokes, along which stacked bars were drawn. The height of each segment within the stacked bar corresponded to the importance of the variable it represented. Different colours were used to distinguish between FDis and FRed. Numbers alongside the grey radial axis denote scale values reflecting normalised importance scores, with the maximum scale adjusted to the highest observed group mean importance score.

environmental stressors. These regions, which are already challenged by arid conditions, are further susceptible to the exacerbating effects of climate oscillations. Across the region spanning from approximately 42°S to 48°S, our results reveal a distinctive ecological setting characterised by high FRed and low FDis, Subantarctic climate, low temperatures and limited species diversity. This region stands out in stark contrast to its northern counterparts, with its harsher climatic conditions contributing to a landscape dominated by few plant species. The observed high FRed and low FDis suggest a prevalence of similar functional traits among coexisting species (Cadotte et al., 2011), indicating convergent adaptation to the harsh environmental conditions, particularly in the latitudes up to approximately 48°S. While this functional similarity allows species to persist under current climates, it also implies that many species occupy similar ecological niches, which increases ecosystem vulnerability to climatic disturbances (Mouillot et al., 2013). If climate change disrupts these niches, it could lead to the simultaneous loss of multiple species that perform overlapping functions, thereby threatening ecosystem functioning. Maintaining current functional biodiversity and improving landscape connectivity should be priorities in conservation to strengthen ecosystem stability and resilience. Between ~ 48°S and ~ 53°S, both FDis and FRed decrease sharply, largely due to naturally low species richness in the high-latitude, cold-adapted forests (e.g., one dominant tree species in TRA forest, two in MAG forest), further exacerbating their susceptibility to environmental change. Therefore, these ecosystems, though low in diversity, are ecologically significant as refugia for cold-adapted species and as reservoirs of unique genetic resources (Morelli et al., 2020), making their conservation under climate change especially critical. The combination of harsh environmental conditions and limited number of species makes it particularly susceptible to climatic shifts and extreme events (Forzieri et al., 2021), pest and disease outbreaks (Estay et al., 2019) and invasive species. Conservation efforts should focus on protecting intact habitats and minimising further disturbances. Our findings highlight the importance of considering functional diversity and redundancy metrics alongside traditional metrics of species richness and abundance in conservation planning, particularly in regions prone to climate extremes.

4.4. Study limitations and future directions

While our study benefits from a broad latitudinal and environmental gradient, we acknowledge that the relatively low number of field plots presents a limitation. The significant relationships observed are likely driven by the substantial ecological variation across the study area, encompassing Mediterranean to cold-temperate climate zones and diverse forest types. Nonetheless, increasing the number of plots, especially in underrepresented areas such as shrublands or transitional forest zones, could improve the resolution and generality of the derived relationships, and may help capture additional patterns and interactions between functional traits and environmental drivers that may not be fully represented with the current sample size. Future studies would benefit from integrating additional sampling efforts, possibly through coordinated long-term ecological networks, to improve the spatial representativeness and robustness of model predictions.

In addition, we used a random 70/30 training–testing split and leave-one-out cross-validation within the training set to evaluate model performance. These approaches are commonly applied in trait prediction and remote sensing studies where field data are limited and sampling is

systematic or random (Camino et al., 2018; Wang et al., 2019; Zhang et al., 2022). While these methods can still be affected by spatial autocorrelation, recent findings suggest that they remain robust under certain conditions (Mushagalusa et al., 2024). We acknowledge, however, that spatial structure remains an important consideration in ecological modelling and have therefore highlighted this issue as a limitation in our study. Future work may benefit from incorporating spatial cross-validation strategies to further improve predictive robustness (Roberts et al., 2017).

5. Conclusion

The large latitudinal gradient we studied serves as an invaluable setting to explore trait-environment relationships and key factors that drive functional trait composition, diversity, and redundancy of tree communities. Our approach provides an opportunity for mapping plant functional traits and assessing plant functional diversity and redundancy at broad scales. We identify a transitional zone, the intermediate latitudinal range between approximately 35°S and 42°S, which may represent a critical threshold where forests with higher resilience to climate change in this region may be found. This is due to the combination of high trait functional diversity and redundancy. The co-occurrence of diverse functional traits and redundant functional groups suggests an ecosystem that possesses both the capacity to adapt to changing conditions and the resilience to withstand disturbances. In the northern region (approximately 30°S to 35°S), high functional diversity but low functional redundancy suggests adaptability to environmental changes but potential vulnerability to species loss. Conservation strategies should prioritise maintaining the local flora to ensure both high functional diversity and redundancy, thereby enhancing the stability of ecosystem functions. Conversely, in the southern region (between approximately 42°S to 48°S), forests exhibit high functional redundancy but low functional diversity, indicating adaptation to harsh Subantarctic conditions. However, the concentration of species with similar traits may increase vulnerability to climate change, as multiple species could be affected by the same disturbance. Conservation efforts should prioritise maintaining existing functional biodiversity and promoting landscape connectivity to support ecosystem stability and forest resilience. From approximately 48°S to 53°S, both functional diversity and redundancy are low, due to extremely low species richness in high-latitude forests. These ecosystems are especially vulnerable to change but remain critical as refugia for cold-adapted species and reservoirs of unique genetic diversity. Conservation should focus on protecting intact habitats and minimising additional disturbance.

CRediT authorship contribution statement

Xiongjie Deng: Writing – review & editing, Writing – original draft, Visualization, Validation, Software, Resources, Methodology, Investigation, Funding acquisition, Formal analysis, Data curation, Conceptualization. **Danny E. Carvajal:** Writing – review & editing, Resources, Methodology, Data curation. **Rocío Urrutia-Jalabert:** Writing – review & editing, Methodology, Data curation. **Waira S. Machida:** Visualization, Methodology. **Alice Rosen:** Writing – review & editing, Visualization. **Huanyuan Zhang-Zheng:** Writing – review & editing, Visualization, Methodology, Investigation. **David Galbraith:** Writing – review & editing, Funding acquisition, Data curation. **Sandra Díaz:** Writing – review & editing. **Yadvinder Malhi:** Writing – review & editing, Supervision, Resources, Project administration, Methodology, Funding acquisition, Data curation. **Jesús Aguirre-Gutiérrez:** Writing – review & editing, Supervision, Resources, Methodology, Funding acquisition, Data curation, Conceptualization.

Declaration of competing interest

The authors declare that they have no known competing financial interests or personal relationships that could have appeared to influence the work reported in this paper.

Acknowledgements

Xiongjie Deng receives the Pay It Forward Scholarship (by China Oxford Scholarship Fund, Oxford) and the New Blackfriars Scholarship (by Blackfriars Hall, Oxford). Danny E. Carvajal is funded by the Fondecyt postdoctoral Grant 3230154 and Proyecto Basal FB210006 (Instituto de Ecología y Biodiversidad, IEB). Rocío Urrutia-Jalabert is funded by the Fondecyt Regular Grant 1240500, the ANID-Millennium Science Initiative-Center Code NCN2024_040, the ANID/FONDAP 1523A0002 project (Center for Climate and Resilience Research CR2). The data collection for this project was funded by the Natural Environment Research Council (NERC) CONICYT ARBOLES project (Grant: NE/S011811/1). Sandra Díaz is funded by an Oxford Martin School Fellowship. Yadvinder Malhi is supported by the Frank Jackson Foundation. Jesús Aguirre-Gutiérrez is funded by the NERC (Grants: NE/T011084/1; NE/Z504191/1), the Leverhulme Trust (RPG-2024-342), and the Royal Society (RG\R1\251370).

Appendix A. Supplementary data

Supplementary data to this article can be found online at https://doi.org/10.1016/j.jag.2025.104704.

Data availability

Data will be made available on request.

References

Abatzoglou, J.T., Dobrowski, S.Z., Parks, S.A., Hegewisch, K.C., 2018. TerraClimate, a high-resolution global dataset of monthly climate and climatic water balance from 1958–2015. Sci. Data 5, 170191. https://doi.org/10.1038/sdata.2017.191.

J. Aguirre-Gutiérrez S.W. Rifai X. Deng H. ter Steege E. Thomson J.J. Corral-Rivas A.F. Guimaraes S. Muller J. Klipel S. Fauset A.F. Resende G. Wallin C.A. Joly K. Abernethy S. Adu-Bredu C. Alexandre Silva E.A. de Oliveira D.R.A. Almeida E. Alvarez-Davila G.P. Asner T.R. Baker M. Benchimol L.P. Bentley E. Berenguer L. Blanc D. Bonal K. Bordin R. Borges de Lima S. Both J. Cabezas Duarte D. Cardoso H. C. de Lima L. Cavalheiro L.A. Cernusak N.C.C. dos Santos Prestes A.C. da Silva Zanzini R.J. da Silva dos Santos Alves da Silva, R., de Andrade Iguatemy, M., De Sousa Oliveira, T.C., Dechant, B., Derroire, G., Dexter, K.G., Rodrigues, D.J., Espírito-Santo, M., Silva, L.F., Domingues, T.F., Ferreira, J., Simon, M.F., Girardin, C.A.J., Hérault, B., Jeffery, K.J., Kalpuzha Ashtamoorthy, S., Kavidapadinjattathil Sivadasan, A., Klitgaard, B., Laurance, W.F., Dan, M.L., Magnusson, W.E., Campos-Filho, E.M., Manoel dos Santos, R., Manzatto, A.G., Silveira, M., Marimon-Junior, B. H., Martin, R.E., Vieira, D.L.M., Metzker, T., Milliken, W., Moonlight, P., Moraes de Seixas, M.M., Morandi, P.S., Muscarella, R., Nava-Miranda, M.G., Nyirambangutse, B., Silva, J.O., Oliveras Menor, I., Francisco Pena Rodrigues, P.J., Pereira de Oliveira, C., Pereira Zanzini, L., Peres, C.A., Punjayil, V., Quesada, C.A., Réjou-Méchain, M., Riutta, T., Rivas-Torres, G., Rosa, C., Salinas, N., Bergamin, R.S., Marimon, B.S., Shenkin, A., Silva Rodrigues, P.M., Figueiredo, A.E.S., Garcia, Q.S., Spósito, T., Storck-Tonon, D., Sullivan, M.J.P., Svátek, M., Vieira Santiago, W.T., Arn Teh, Y., Theruvil Parambil Sivan, P., Nascimento, M.T., Veenendaal, E., Zo-Bi, I.C., Dago, M. R., Traoré, S., Patacca, M., Badouard, V., de Padua Chaves e Carvalho, S., White, L.J. T., Zhang-Zheng, H., Zibera, E., Zwerts, J.A., Burslem, D.F.R.P., Silman, M., Chave, J., Enquist, B.J., Barlow, J., Phillips, O.L., Coomes, D.A., Malhi, Y., Canopy functional trait variation across Earth's tropical forests Nature 1–8 2025 10.1038/s41586-025-08663-2.

Araya-Osses, D., Casanueva, A., Román-Figueroa, C., Uribe, J.M., Paneque, M., 2020. Climate change projections of temperature and precipitation in Chile based on statistical downscaling. Clim. Dyn. 54, 4309–4330.

Asner, G.P., Martin, R.E., Knapp, D.E., Tupayachi, R., Anderson, C.B., Sinca, F., Vaughn, N.R., Llactayo, W., 2017. Airborne laser-guided imaging spectroscopy to map forest trait diversity and guide conservation. Science 355, 385–389. https://doi.org/10.1126/science.aaj1987.

Bjorkman, A.D., Myers-Smith, I.H., Elmendorf, S.C., Normand, S., Rüger, N., Beck, P.S.A., Blach-Overgaard, A., Blok, D., Cornelissen, J.H.C., Forbes, B.C., Georges, D., Goetz, S.J., Guay, K.C., Henry, G.H.R., HilleRisLambers, J., Hollister, R.D., Karger, D. N., Kattge, J., Manning, P., Prevéy, J.S., Rixen, C., Schaepman-Strub, G., Thomas, H. J.D., Vellend, M., Wilmking, M., Wipf, S., Carbognani, M., Hermanutz, L.,

Lévesque, E., Molau, U., Petraglia, A., Soudzilovskaia, N.A., Spasojevic, M.J., Tomaselli, M., Vowles, T., Alatalo, J.M., Alexander, H.D., Anadon-Rosell, A., Angers-Blondin, S., te Beest, M., Berner, L., Björk, R.G., Buchwal, A., Buras, A., Christie, K., Cooper, E.J., Dullinger, S., Elberling, B., Eskelinen, A., Frei, E.R., Grau, O., Grogan, P., Hallinger, M., Harper, K.A., Heijmans, M.M.P.D., Hudson, J., Hülber, K., Iturrate-Garcia, M., Iversen, C.M., Jaroszynska, F., Johnstone, J.F., Jørgensen, R.H., Kaarlejärvi, E., Klady, R., Kuleza, S., Kulonen, A., Lamarque, L.J., Lantz, T., Little, C. J., Speed, J.D.M., Michelsen, A., Milbau, A., Nabe-Nielsen, J., Nielsen, S.S., Ninot, J. M., Oberbauer, S.F., Olofsson, J., Onipchenko, V.G., Rumpf, S.B., Semenchuk, P., Shetti, R., Collier, L.S., Street, L.E., Suding, K.N., Tape, K.D., Trant, A., Treier, U.A., Tremblay, J.-P., Tremblay, M., Venn, S., Weijers, S., Zamin, T., Boulanger-Lapointe, N., Gould, W.A., Hik, D.S., Hofgaard, A., Jónsdóttir, I.S., Jorgenson, J., Klein, J., Magnusson, B., Tweedie, C., Wookey, P.A., Bahn, M., Blonder, B., van Bodegom, P.M., Bond-Lamberty, B., Campetella, G., Cerabolini, B.E.L., Chapin, F.S., Cornwell, W.K., Craine, J., Dainese, M., de Vries, F.T., Díaz, S., Enquist, B.J., Green, W., Milla, R., Niinemets, Ü., Onoda, Y., Ordoñez, J.C., Ozinga, W.A., Penuelas, J., Poorter, H., Poschlod, P., Reich, P.B., Sandel, B., Schamp, B., Sheremetev, S., Weiher, E., 2018. Plant functional trait change across a warming tundra biome. Nature 562, 57–62. https://doi.org/10.1038/s41586-018-0563-7.

Bowman, D.M., Moreira-Muñoz, A., Kolden, C.A., Chávez, R.O., Muñoz, A.A., Salinas, F., González-Reyes, Á., Rocco, R., De la Barrera, F., Williamson, G.J., 2019. Human–environmental drivers and impacts of the globally extreme 2017 chilean fires. Ambio 48, 350–362.

Braun, A.C., Troeger, D., Garcia, R., Aguayo, M., Barra, R., Vogt, J., 2017. Assessing the impact of plantation forestry on plant biodiversity: a comparison of sites in Central Chile and chilean Patagonia. Glob. Ecol. Conserv. 10, 159–172.

Breiman, L., 2001. Random forests. Mach. Learn. 45, 5–32.

Bruelheide, H., Dengler, J., Purschke, O., Lenoir, J., Jiménez-Alfaro, B., Hennekens, S.M., Botta-Dukát, Z., Chytrý, M., Field, R., Jansen, F., Kattge, J., Pillar, V.D., Schrodt, F., Mahecha, M.D., Peet, R.K., Sandel, B., van Bodegom, P., Altman, J., Alvarez-Dávila, E., Arfin Khan, M.A.S., Attorre, F., Aubin, I., Baraloto, C., Barroso, J.G., Bauters, M., Bergmeier, E., Biurrun, I., Bjorkman, A.D., Blonder, B., Čarni, A., Cayuela, L., Černý, T., Cornelissen, J.H.C., Craven, D., Dainese, M., Derroire, G., De Sanctis, M., Díaz, S., Doležal, J., Farfan-Rios, W., Feldpausch, T.R., Fenton, N.J., Garnier, E., Guerin, G.R., Gutiérrez, A.G., Haider, S., Hattab, T., Henry, G., Hérault, B., Higuchi, P., Hölzel, N., Homeier, J., Jentsch, A., Jürgens, N., Kącki, Z., Karger, D.N., Kessler, M., Kleyer, M., Knollová, I., Korolyuk, A.Y., Kühn, I., Laughlin, D.C., Lens, F., Loos, J., Louault, F., Lyubenova, M.I., Malhi, Y., Marcenò, C., Mencuccini, M., Müller, J.V., Munzinger, J., Myers-Smith, I.H., Neill, D. A., Niinemets, Ü., Orwin, K.H., Ozinga, W.A., Penuelas, J., Pérez-Haase, A., Petřík, P., Phillips, O.L., Pärtel, M., Reich, P.B., Römermann, C., Rodrigues, A.V., Sabatini, F.M., Sardans, J., Schmidt, M., Seidler, G., Silva Espejo, J.E., Silveira, M., Smyth, A., Sporbert, M., Svenning, J.-C., Tang, Z., Thomas, R., Tsiripidis, I., Vassilev, K., Violle, C., Virtanen, R., Weiher, E., Welk, E., Wesche, K., Winter, M., Wirth, C., Jandt, U., 2018. Global trait–environment relationships of plant communities. Nat. Ecol. Evol. 2, 1906–1917. https://doi.org/10.1038/s41559-018-0699-8.

Butler, E.E., Datta, A., Flores-Moreno, H., Chen, M., Wythers, K.R., Fazayeli, F., Banerjee, A., Atkin, O.K., Kattge, J., Amiaud, B., 2017. Mapping local and global variability in plant trait distributions. Proc. Natl. Acad. Sci. 114, E10937–E10946.

Cadotte, M., Albert, C.H., Walker, S.C., 2013. The ecology of differences: assessing community assembly with trait and evolutionary distances. Ecol. Lett. 16, 1234–1244.

Cadotte, M.W., Carscadden, K., Mirotchnick, N., 2011. Beyond species: functional diversity and the maintenance of ecological processes and services. J. Appl. Ecol. 48, 1079–1087.

Camarretta, N., A. Harrison, P., Lucieer, A., M. Potts, B., Davidson, N., Hunt, M., 2020. From Drones to Phenotype: Using UAV-LiDAR to Detect Species and Provenance Variation in Tree Productivity and Structure. Remote Sens. 12, 3184. https://doi.org/10.3390/rs12193184.

Camino, C., González-Dugo, V., Hernández, P., Sillero, J.C., Zarco-Tejada, P.J., 2018. Improved nitrogen retrievals with airborne-derived fluorescence and plant traits quantified from VNIR-SWIR hyperspectral imagery in the context of precision agriculture. Int. J. Appl. Earth Obs. Geoinformation 70, 105–117. https://doi.org/10.1016/j.jag.2018.04.013.

Candeias, M., Fraterrigo, J., 2020. Trait coordination and environmental filters shape functional trait distributions of forest understory herbs. Ecol. Evol. 10, 14098–14112.

Cardinale, B.J., Duffy, J.E., Gonzalez, A., Hooper, D.U., Perrings, C., Venail, P., Narwani, A., Mace, G.M., Tilman, D., Wardle, D.A., 2012. Biodiversity loss and its impact on humanity. Nature 486, 59–67.

Carmona, C.P., De Bello, F., Mason, N.W.H., Lepš, J., 2016. Traits without Borders: integrating functional diversity across scales. Trends Ecol. Evol. 31, 382–394. https://doi.org/10.1016/j.tree.2016.02.003.

Cavieres, L.A., Badano, E.I., Sierra-Almeida, A., Molina-Montenegro, M.A., 2007. Microclimatic modifications of cushion plants and their consequences for seedling survival of native and non-native herbaceous species in the high Andes of central Chile. Arct. Antarct. Alp. Res. 39, 229–236.

Chen, J., Shao, Z., Deng, X., Huang, X., Dang, C., 2023. Vegetation as the catalyst for water circulation on global terrestrial ecosystem. Sci. Total Environ. 895, 165071. https://doi.org/10.1016/j.scitotenv.2023.165071.

Cordero, R.R., Feron, S., Damiani, A., Carrasco, J., Karas, C., Wang, C., Kraamwinkel, C. T., Beaulieu, A., 2024. Extreme fire weather in Chile driven by climate change and el niño–southern oscillation (ENSO). Sci. Rep. 14, 1974. https://doi.org/10.1038/s41598-024-52481-x.

Correia, D.L.P., Raulier, F., Bouchard, M., Filotas, É., 2018. Response diversity, functional redundancy, and post-logging productivity in northern temperate and boreal forests. Ecol. Appl. 28, 1282–1291. https://doi.org/10.1002/eap.1727.

Costa-Saura, J.M., Martínez-Vilalta, J., Trabucco, A., Spano, D., Mereu, S., 2016. Specific leaf area and hydraulic traits explain niche segregation along an aridity gradient in Mediterranean woody species. Perspect. Plant Ecol. Evol. Syst. 21, 23–30.

Cueto, D.A., Alaniz, A.J., Hidalgo-Corrotea, C., Vergara, P.M., Carvajal, M.A., Barrios-Saravia, A., 2025. Chilean Mediterranean forest on the verge of collapse? evidence from a comprehensive risk analysis. Sci. Total Environ. 964, 178557. https://doi.org/10.1016/j.scitotenv.2025.178557.

De la Barrera, F., Barraza, F., Favier, P., Ruiz, V., Quense, J., 2018. Megafires in Chile 2017: monitoring multiscale environmental impacts of burned ecosystems. Sci. Total Environ. 637, 1526–1536.

Dell, A.I., Pawar, S., Savage, V.M., 2011. Systematic variation in the temperature dependence of physiological and ecological traits. Proc. Natl. Acad. Sci. 108, 10591–10596.

Denelle, P., Violle, C., Munoz, F., 2019. Distinguishing the signatures of local environmental filtering and regional trait range limits in the study of trait–environment relationships. Oikos 128, 960–971.

Díaz, S., Lavorel, S., De Bello, F., Quétier, F., Grigulis, K., Robson, T.M., 2007. Incorporating plant functional diversity effects in ecosystem service assessments. Proc. Natl. Acad. Sci. 104, 20684–20689.

Díaz, S., Purvis, A., Cornelissen, J.H.C., Mace, G.M., Donoghue, M.J., Ewers, R.M., Jordano, P., Pearse, W.D., 2013. Functional traits, the phylogeny of function, and ecosystem service vulnerability. Ecol. Evol. 3, 2958–2975. https://doi.org/10.1002/ece3.601.

Donohue, I., Hillebrand, H., Montoya, J.M., Petchey, O.L., Pimm, S.L., Fowler, M.S., Healy, K., Jackson, A.L., Lurgi, M., McClean, D., 2016. Navigating the complexity of ecological stability. Ecol. Lett. 19, 1172–1185.

Drusch, M., Del Bello, U., Carlier, S., Colin, O., Fernandez, V., Gascon, F., Hoersch, B., Isola, C., Laberinti, P., Martimort, P., 2012. Sentinel-2: ESA's optical high-resolution mission for GMES operational services. Remote Sens. Environ. 120, 25–36.

Echeverría, C., Coomes, D., Salas, J., Rey-Benayas, J.M., Lara, A., Newton, A., 2006. Rapid deforestation and fragmentation of chilean temperate forests. Biol. Conserv. 130, 481–494.

Echeverría-Londoño, S., Enquist, B.J., Neves, D.M., Violle, C., Boyle, B., Kraft, N.J., Maitner, B.S., McGill, B., Peet, R.K., Sandel, B., 2018. Plant functional diversity and the biogeography of biomes in north and South America. Front. Ecol. Evol. 6, 219.

Ellis, C.J., Eaton, S., 2021. Microclimates hold the key to spatial forest planning under climate change: cyanolichens in temperate rainforest. Glob. Change Biol. 27, 1915–1926.

Estay, S.A., Chávez, R.O., Rocco, R., Gutiérrez, A.G., 2019. Quantifying massive outbreaks of the defoliator moth ormiscodes amphimone in deciduous Nothofagus-dominated southern forests using remote sensing time series analysis. J. Appl. Entomol. 143, 787–796.

Farr, T.G., Rosen, P.A., Caro, E., Crippen, R., Duren, R., Hensley, S., Kobrick, M., Paller, M., Rodriguez, E., Roth, L., 2007. The shuttle radar topography mission. Rev, Geophys, p. 45.

Fisher, J.B., Lee, B., Purdy, A.J., Halverson, G.H., Dohlen, M.B., Cawse-Nicholson, K., Wang, A., Anderson, R.G., Aragon, B., Arain, M.A., Baldocchi, D.D., Baker, J.M., Barral, H., Bernacchi, C.J., Bernhofer, C., Biraud, S.C., Bohrer, G., Brunsell, N., Cappelaere, B., Castro-Contreras, S., Chun, J., Conrad, B.J., Cremonese, E., Demarty, J., Desai, A.R., De Ligne, A., Foltýnová, L., Goulden, M.L., Griffis, T.J., Grünwald, T., Johnson, M.S., Kang, M., Kelbe, D., Kowalska, N., Lim, J.-H., Maïnassara, I., McCabe, M.F., Missik, J.E.C., Mohanty, B.P., Moore, C.E., Morillas, L., Morrison, R., Munger, J.W., Posse, G., Richardson, A.D., Russell, E.S., Ryu, Y., Sanchez-Azofeifa, A., Schmidt, M., Schwartz, E., Sharp, I., Šigut, L., Tang, Y., Hulley, G., Anderson, M., Hain, C., French, A., Wood, E., Hook, S., 2020. ECOSTRESS: NASA's next generation Mission to measure Evapotranspiration from the international Space Station. water resour. Res. 56, e2019WR026058. https://doi.org/10.1029/2019WR026058.

Folke, C., Carpenter, S., Walker, B., Scheffer, M., Elmqvist, T., Gunderson, L., Holling, C. S., 2004. Regime shifts, resilience, and biodiversity in ecosystem management. Annu. Rev. Ecol. Evol. Syst. 35, 557–581.

Fortunel, C., Paine, C.E.T., Fine, P.V.A., Kraft, N.J.B., Baraloto, C., 2014. Environmental factors predict community functional composition in amazonian forests. J. Ecol. 102, 145–155. https://doi.org/10.1111/1365-2745.12160.

Forzieri, G., Girardello, M., Ceccherini, G., Spinoni, J., Feyen, L., Hartmann, H., Beck, P. S., Camps-Valls, G., Chirici, G., Mauri, A., 2021. Emergent vulnerability to climate-driven disturbances in european forests. Nat. Commun. 12, 1081.

Gámez-Virués, S., Perović, D.J., Gossner, M.M., Börschig, C., Blüthgen, N., De Jong, H., Simons, N.K., Klein, A.-M., Krauss, J., Maier, G., 2015. Landscape simplification filters species traits and drives biotic homogenization. Nat. Commun. 6, 8568.

Garreaud, R.D., Boisier, J.P., Rondanelli, R., Montecinos, A., Sepúlveda, H.H., Veloso-Aguila, D., 2020. The central Chile mega drought (2010–2018): a climate dynamics perspective. Int. J. Climatol. 40, 421–439.

Gitelson, A., Merzlyak, M.N., 1994. Spectral reflectance changes associated with autumn senescence of *Aesculus hippocastanum* L. and *Acer platanoides* L. leaves. spectral features and relation to chlorophyll estimation. J. Plant Physiol. 143, 286–292. https://doi.org/10.1016/S0176-1617(11)81633-0.

Gorelick, N., Hancher, M., Dixon, M., Ilyushchenko, S., Thau, D., Moore, R., 2017. Google Earth engine: Planetary-scale geospatial analysis for everyone. Remote Sens. Environ. 202, 18–27. https://doi.org/10.1016/j.rse.2017.06.031.

Grime, J.P., 2006. Trait convergence and trait divergence in herbaceous plant communities: mechanisms and consequences. J. Veg. Sci. 17, 255–260.

Hauser, L.T., Féret, J.-B., An Binh, N., Van Der Windt, N., Sil, Â.F., Timmermans, J., Soudzilovskaia, N.A., Van Bodegom, P.M., 2021. Towards scalable estimation of plant functional diversity from Sentinel-2: in-situ validation in a heterogeneous (semi-)natural landscape. Remote Sens. Environ. 262, 112505. https://doi.org/10.1016/j.rse.2021.112505.

Helfenstein, I.S., Schneider, F.D., Schaepman, M.E., Morsdorf, F., 2022. Assessing biodiversity from space: impact of spatial and spectral resolution on trait-based functional diversity. Remote Sens. Environ. 275, 113024. https://doi.org/10.1016/j.rse.2022.113024.

Hengl, T., Mendes de Jesus, J., Heuvelink, G.B., Ruiperez Gonzalez, M., Kilibarda, M., Blagotić, A., Shangguan, W., Wright, M.N., Geng, X., Bauer-Marschallinger, B., 2017. SoilGrids250m: global gridded soil information based on machine learning. PLoS One 12, e0169748.

Hooper, D.U., Chapin III, F.S., Ewel, J.J., Hector, A., Inchausti, P., Lavorel, S., Lawton, J. H., Lodge, D.M., Loreau, M., Naeem, S., 2005. Effects of biodiversity on ecosystem functioning: a consensus of current knowledge. Ecol. Monogr. 75, 3–35.

Hortal, J., de Bello, F., Diniz-Filho, J.A.F., Lewinsohn, T.M., Lobo, J.M., Ladle, R.J., 2015. Seven shortfalls that beset large-scale knowledge of biodiversity. Annu. Rev. Ecol. Evol. Syst. 46, 523–549.

Huertas Herrera, A., Toro-Manríquez, M.D.R., Salinas Sanhueza, J., Rivas Guíñez, F., Lencinas, M.V., Martínez Pastur, G., 2023. Relationships among livestock, structure, and regeneration in chilean austral macrozone temperate forests. Trees for. People 13, 100426. https://doi.org/10.1016/j.tfp.2023.100426.

Huete, A.R., 1988. A soil-adjusted vegetation index (SAVI). Remote Sens. Environ. 25, 295–309. https://doi.org/10.1016/0034-4257(88)90106-X.

Hussain, S., Gao, K., Din, M., Gao, Y., Shi, Z., Wang, S., 2020. Assessment of UAV-Onboard multispectral sensor for non-destructive site-specific rapeseed crop phenotype Variable at different phenological stages and resolutions. Remote Sens. 12, 397. https://doi.org/10.3390/rs12030397.

Isbell, F., Craven, D., Connolly, J., Loreau, M., Schmid, B., Beierkuhnlein, C., Bezemer, T. M., Bonin, C., Bruelheide, H., De Luca, E., 2015. Biodiversity increases the resistance of ecosystem productivity to climate extremes. Nature 526, 574–577.

Isbell, F., Gonzalez, A., Loreau, M., Cowles, J., Díaz, S., Hector, A., Mace, G.M., Wardle, D.A., O'Connor, M.I., Duffy, J.E., 2017. Linking the influence and dependence of people on biodiversity across scales. Nature 546, 65–72.

Jetz, W., Cavender-Bares, J., Pavlick, R., Schimel, D., Davis, F.W., Asner, G.P., Guralnick, R., Kattge, J., Latimer, A.M., Moorcroft, P., 2016. Monitoring plant functional diversity from space. Nat. Plants 2, 1–5.

Kaiser, J., Schefuß, E., Lamy, F., Mohtadi, M., Hebbeln, D., 2008. Glacial to holocene changes in sea surface temperature and coastal vegetation in north central Chile: high *versus* low latitude forcing. Quat. Sci. Rev. 27, 2064–2075. https://doi.org/10.1016/j.quascirev.2008.08.025.

Kamoske, A.G., Dahlin, K.M., Serbin, S.P., Stark, S.C., 2021. Leaf traits and canopy structure together explain canopy functional diversity: an airborne remote sensing approach. Ecol. Appl. 31, e02230. https://doi.org/10.1002/eap.2230.

Kergunteuil, A., Humair, L., Münzbergová, Z., Rasmann, S., 2019. Plant adaptation to different climates shapes the strengths of chemically mediated tritrophic interactions. Funct. Ecol. 33, 1893–1903.

Kier, G., Mutke, J., Dinerstein, E., Ricketts, T.H., Küper, W., Kreft, H., Barthlott, W., 2005. Global patterns of plant diversity and floristic knowledge. J. Biogeogr. 32, 1107–1116. https://doi.org/10.1111/j.1365-2699.2005.01272.x.

Kraft, N.J., Godoy, O., Levine, J.M., 2015. Plant functional traits and the multidimensional nature of species coexistence. Proc. Natl. Acad. Sci. 112, 797–802.

Krishnadas, M., Beckman, N.G., Zuluaga, J.C.P., Zhu, Y., Whitacre, J., Wenzel, J.W., Queenborough, S.A., Comita, L.S., 2018. Environment and past land use together predict functional diversity in a temperate forest. Ecol. Appl. 28, 2142–2152. https://doi.org/10.1002/eap.1802.

Kuhn, M., 2008. Building predictive models in R using the caret package. J. Stat. Softw. 28, 1–26. https://doi.org/10.18637/jss.v028.i05.

Laliberté, E., Legendre, P., 2010. A distance-based framework for measuring functional diversity from multiple traits. Ecology 91, 299–305. https://doi.org/10.1890/08-2244.1.

Laliberté, E., Legendre, P., Shipley, B., Laliberté, M.E., 2014. Package 'fd.' meas. Funct. Divers. Mult. Traits Tools Funct. Ecol. 1, 12.

Laughlin, D.C., Strahan, R.T., Adler, P.B., Moore, M.M., 2018. Survival rates indicate that correlations between community-weighted mean traits and environments can be unreliable estimates of the adaptive value of traits. Ecol. Lett. 21, 411–421.

Le Roux, J.P., 2012. A review of Tertiary climate changes in southern South America and the Antarctic peninsula. Part 2: continental conditions. Sediment. Geol. 247–248, 21–38. https://doi.org/10.1016/j.sedgeo.2011.12.001.

Ma, X., Mahecha, M.D., Migliavacca, M., van der Plas, F., Benavides, R., Ratcliffe, S., Kattge, J., Richter, R., Musavi, T., Baeten, L., Barnoaiea, I., Bohn, F.J., Bouriaud, O., Bussotti, F., Coppi, A., Domisch, T., Huth, A., Jaroszewicz, B., Joswig, J., Pabon-Moreno, D.E., Papale, D., Selvi, F., Laurin, G.V., Valladares, F., Reichstein, M., Wirth, C., 2019. Inferring plant functional diversity from space: the potential of Sentinel-2. Remote Sens. Environ. 233, 111368. https://doi.org/10.1016/j.rse.2019.111368.

Malhi, Y., Aragão, L.E.O.C., Galbraith, D., Huntingford, C., Fisher, R., Zelazowski, P., Sitch, S., McSweeney, C., Meir, P., 2009. Exploring the likelihood and mechanism of a climate-change-induced dieback of the Amazon rainforest. Proc. Natl. Acad. Sci. 106, 20610–20615. https://doi.org/10.1073/pnas.0804619106.

Malhi, Y., Baldocchi, D., Jarvis, P., 1999. The carbon balance of tropical, temperate and boreal forests. Plant Cell Environ. 22, 715–740.

Malhi, Y., Christmann, T., Deng, X., Zhang-Zheng, H., Moore, S., Riutta, T., 2024. Forest carbon budgets and climate change, in: Routledge Handbook of Forest Ecology. Routledge.

Meyer, J., Kröncke, I., 2019. Shifts in trait-based and taxonomic macrofauna community structure along a 27-year time-series in the south-eastern North Sea. PLoS One 14, e0226410. https://doi.org/10.1371/journal.pone.0226410.

Miranda, A., Altamirano, A., Cayuela, L., Lara, A., González, M., 2017. Native forest loss in the chilean biodiversity hotspot: revealing the evidence. Reg. Environ. Change 17, 285–297. https://doi.org/10.1007/s10113-016-1010-7.

Miranda, A., Syphard, A.D., Berdugo, M., Carrasco, J., Gómez-González, S., Ovalle, J.F., Delpiano, C.A., Vargas, S., Squeo, F.A., Miranda, M.D., Dobbs, C., Mentler, R., Lara, A., Garreaud, R., 2023. Widespread synchronous decline of Mediterranean-type forest driven by accelerated aridity. Nat. Plants 9, 1810–1817. https://doi.org/10.1038/s41477-023-01541-7.

Morelli, T.L., Barrows, C.W., Ramirez, A.R., Cartwright, J.M., Ackerly, D.D., Eaves, T.D., Ebersole, J.L., Krawchuk, M.A., Letcher, B.H., Mahalovich, M.F., Meigs, G.W., Michalak, J.L., Millar, C.I., Quiñones, R.M., Stralberg, D., Thorne, J.H., 2020. Climate-change refugia: biodiversity in the slow lane. Front. Ecol. Environ. 18, 228–234. https://doi.org/10.1002/fee.2189.

Mouchet, M.A., Villéger, S., Mason, N.W.H., Mouillot, D., 2010. Functional diversity measures: an overview of their redundancy and their ability to discriminate community assembly rules. Funct. Ecol. 24, 867–876. https://doi.org/10.1111/j.1365-2435.2010.01695.x.

Mouillot, D., Graham, N.A.J., Villéger, S., Mason, N.W.H., Bellwood, D.R., 2013. A functional approach reveals community responses to disturbances. Trends Ecol. Evol. 28, 167–177. https://doi.org/10.1016/j.tree.2012.10.004.

Mushagalusa, C.A., Fandohan, A.B., Glèlè Kakaï, R., 2024. Random forest and spatial cross-validation performance in predicting species abundance distributions. Environ. Syst. Res. 13, 23. https://doi.org/10.1186/s40068-024-00352-9.

Myers, N., Mittermeier, R.A., Mittermeier, C.G., da Fonseca, G.A.B., Kent, J., 2000. Biodiversity hotspots for conservation priorities. Nature 403, 853–858. https://doi.org/10.1038/35002501.

Myneni, R.B., Hall, F.G., Sellers, P.J., Marshak, A.L., 1995. The interpretation of spectral vegetation indexes. IEEE Trans. Geosci. Remote Sens. 33, 481–486. https://doi.org/10.1109/TGRS.1995.8746029.

Nahuelhual, L., Donoso, P., Lara, A., Núñez, D., Oyarzún, C., Neira, E., 2007. VALUING ECOSYSTEM SERVICES OF CHILEAN TEMPERATE RAINFORESTS. Environ. Dev. Sustain. 9, 481–499. https://doi.org/10.1007/s10668-006-9033-8.

Oliver, T.H., Heard, M.S., Isaac, N.J.B., Roy, D.B., Procter, D., Eigenbrod, F., Freckleton, R., Hector, A., Orme, C.D.L., Petchey, O.L., Proença, V., Raffaelli, D., Suttle, K.B., Mace, G.M., Martín-López, B., Woodcock, B.A., Bullock, J.M., 2015. Biodiversity and resilience of ecosystem functions. Trends Ecol. Evol. 30, 673–684. https://doi.org/10.1016/j.tree.2015.08.009.

Pavoine, S., 2020. adiv: an r package to analyse biodiversity in ecology. Methods Ecol. Evol. 11, 1106–1112. https://doi.org/10.1111/2041-210X.13430.

Pérez, C.A., Armesto, J.J., Torrealba, C., Carmona, M.R., 2003. Litterfall dynamics and nitrogen use efficiency in two evergreen temperate rainforests of southern Chile. Austral Ecol. 28, 591–600. https://doi.org/10.1046/j.1442-9993.2003.01315.x.

Perez-Quezada, J.F., Barichivich, J., Urrutia-Jalabert, R., Carrasco, E., Aguilera, D., Bacour, C., Lara, A., 2023. Warming and drought weaken the Carbon sink capacity of an endangered paleoendemic temperate rainforest in South America. J. Geophys. res. Biogeosciences 128, e2022JG007258. https://doi.org/10.1029/2022JG007258.

Perez-Quezada, J.F., Urrutia, P., Olivares-Rojas, J., Meijide, A., Sánchez-Cañete, E.P., Gaxiola, A., 2021. Long term effects of fire on the soil greenhouse gas balance of an old-growth temperate rainforest. Sci. Total Environ. 755, 142442. https://doi.org/10.1016/j.scitotenv.2020.142442.

Pla, L., Casanoves, F., Di Rienzo, J., 2012. Quantifying Functional Biodiversity, SpringerBriefs in Environmental Science. Springer Netherlands, Dordrecht. https://doi.org/10.1007/978-94-007-2648-2.

Poorter, H., Niinemets, Ü., Poorter, L., Wright, I.J., Villar, R., 2009. Causes and consequences of variation in leaf mass per area (LMA): a meta-analysis. New Phytol. 182, 565–588. https://doi.org/10.1111/j.1469-8137.2009.02830.x.

Potapov, P., Li, X., Hernandez-Serna, A., Tyukavina, A., Hansen, M.C., Kommareddy, A., Pickens, A., Turubanova, S., Tang, H., Silva, C.E., Armston, J., Dubayah, R., Blair, J. B., Hofton, M., 2021. Mapping global forest canopy height through integration of GEDI and landsat data. Remote Sens. Environ. 253, 112165. https://doi.org/10.1016/j.rse.2020.112165.

Qi, J., Chehbouni, A., Huete, A.R., Kerr, Y.H., Sorooshian, S., 1994. A modified soil adjusted vegetation index. Remote Sens. Environ. 48, 119–126. https://doi.org/10.1016/0034-4257(94)90134-1.

Quick, D.J., Chadwick, O.A., 2011. Accumulation of salt-rich dust from Owens Lake playa in nearby alluvial soils. aeolian res. AGU Fall Meeting Session on Aeolian Dust: Transport Processes, Anthropogenic Forces and Biogeochemical Cycling 3, 23–29. https://doi.org/10.1016/j.aeolia.2011.03.004.

Ricotta, C., De Bello, F., Moretti, M., Caccianiga, M., Cerabolini, B.E.L., Pavoine, S., 2016. Measuring the functional redundancy of biological communities: a quantitative guide. Methods Ecol. Evol. 7, 1386–1395. https://doi.org/10.1111/2041-210X.12604.

Roberts, D.R., Bahn, V., Ciuti, S., Boyce, M.S., Elith, J., Guillera-Arroita, G., Hauenstein, S., Lahoz-Monfort, J.J., Schröder, B., Thuiller, W., Warton, D.I., Wintle, B.A., Hartig, F., Dormann, C.F., 2017. Cross-validation strategies for data with temporal, spatial, hierarchical, or phylogenetic structure. Ecography 40, 913–929. https://doi.org/10.1111/ecog.02881.

Rosenfeld, J.S., 2002. Functional redundancy in ecology and conservation. Oikos 98, 156–162. https://doi.org/10.1034/j.1600-0706.2002.980116.x.

Rouault, E., Warmerdam, F., Schwehr, K., Kiselev, A., Butler, H., Łoskot, M., Szekeres, T., Tourigny, E., Landa, M., Miara, I., Elliston, B., Chaitanya, K., Plesea, L., Morissette, D., Jolma, A., Dawson, N., Baston, D., de Stigter, C., Miura, H., 2024. GDAL. Zenodo. https://doi.org/10.5281/zenodo.13330875.

Rozzi, R., Rosenfeld, S., Armesto, J.J., Mansilla, A., Núñez-Ávila, M., Massardo, F., 2023. Ecological connections across the Marine-Terrestrial Interface in chilean Patagonia. In: Castilla, J.C., Armesto Zamudio, J.J., Martínez-Harms, M.J., Tecklin, D. (Eds.), Conservation in Chilean Patagonia: Assessing the State of Knowledge, Opportunities, and Challenges. Springer International Publishing, Cham, pp. 323–354. https://doi.org/10.1007/978-3-031-39408-9_13.

Ruiz-Benito, P., Ratcliffe, S., Jump, A.S., Gómez-Aparicio, L., Madrigal-González, J., Wirth, C., Kändler, G., Lehtonen, A., Dahlgren, J., Kattge, J., Zavala, M.A., 2017. Functional diversity underlies demographic responses to environmental variation in european forests. Glob. Ecol. Biogeogr. 26, 128–141. https://doi.org/10.1111/geb.12515.

Sarricolea, P., Herrera-Ossandon, M., Meseguer-Ruiz, Ó., 2017. Climatic regionalisation of continental Chile. J. Maps 13, 66–73. https://doi.org/10.1080/17445647.2016.1259592.

Schmitt, S., Hérault, B., Ducouret, É., Baranger, A., Tysklind, N., Heuertz, M., Marcon, É., Cazal, S.O., Derroire, G., 2020. Topography consistently drives intra- and inter-specific leaf trait variation within tree species complexes in a neotropical forest. Oikos 129, 1521–1530. https://doi.org/10.1111/oik.07488.

Schneider, F.D., Morsdorf, F., Schmid, B., Petchey, O.L., Hueni, A., Schimel, D.S., Schaepman, M.E., 2017. Mapping functional diversity from remotely sensed morphological and physiological forest traits. Nat. Commun. 8, 1441. https://doi.org/10.1038/s41467-017-01530-3.

Sheffield, J., Wood, E.F., Pan, M., Beck, H., Coccia, G., Serrat-Capdevila, A., Verbist, K., 2018. Satellite remote sensing for water resources Management: potential for supporting Sustainable development in data-poor regions. Water Resour. Res. 54, 9724–9758. https://doi.org/10.1029/2017WR022437.

Smith-Ramírez, C., 2004. The chilean coastal range: a vanishing center of biodiversity and endemism in south American temperate rainforests. Biodivers. Conserv. 13, 373–393. https://doi.org/10.1023/B:BIOC.0000006505.67560.9f.

Suding, K.N., Lavorel, S., Chapin Iii, F.S., Cornelissen, J.H.C., Díaz, S., Garnier, E., Goldberg, D., Hooper, D.U., Jackson, S.T., Navas, M.-L., 2008. Scaling environmental change through the community-level: a trait-based response-and-effect framework for plants. Glob. Change Biol. 14, 1125–1140. https://doi.org/10.1111/j.1365-2486.2008.01557.x.

Sun, W., Chen, D., Li, Z., Li, S., Cheng, S., Niu, X., Cai, Y., Shi, Z., Wu, C., Yang, G., Yang, X., 2024. Monitoring wetland plant diversity from space: Progress and perspective. Int. J. Appl. Earth Obs. Geoinformation 130, 103943. https://doi.org/10.1016/j.jag.2024.103943.

Tecklin, D., DellaSala, D.A., Luebert, F., Pliscoff, P., 2011. Valdivian Temperate Rainforests of Chile and Argentina, in: DellaSala, D.A. (Ed.), Temperate and Boreal Rainforests of the World: Ecology and Conservation. Island Press/Center for Resource Economics, Washington, DC, pp. 132–153. https://doi.org/10.5822/978-1-61091-008-8_5.

Thomson, E.R., Spiegel, M.P., Althuizen, I.H.J., Bass, P., Chen, S., Chmurzynski, A., Halbritter, A.H., Henn, J.J., Jónsdóttir, I.S., Klanderud, K., Li, Y., Maitner, B.S., Michaletz, S.T., Niittynen, P., Roos, R.E., Telford, R.J., Enquist, B.J., Vandvik, V., Macias-Fauria, M., Malhi, Y., 2021. Multiscale mapping of plant functional groups and plant traits in the high Arctic using field spectroscopy, UAV imagery and sentinel-2A data. Environ. Res. Lett. 16, 055006. https://doi.org/10.1088/1748-9326/abf464.

Urrutia-Jalabert, R., Malhi, Y., Barichivich, J., Lara, A., Delgado-Huertas, A., Rodríguez, C.G., Cuq, E., 2015a. Increased water use efficiency but contrasting tree growth patterns in Fitzroya cupressoides forests of southern Chile during recent decades. J. Geophys. Res. Biogeosciences 120, 2505–2524. https://doi.org/10.1002/2015JG003098.

Urrutia-Jalabert, R., Malhi, Y., Lara, A., 2015b. The oldest, slowest rainforests in the world? massive biomass and slow Carbon dynamics of Fitzroya cupressoides temperate forests in southern Chile. PLoS One 10, e0137569. https://doi.org/10.1371/journal.pone.0137569.

Vilà-Cabrera, A., Martínez-Vilalta, J., Retana, J., 2015. Functional trait variation along environmental gradients in temperate and Mediterranean trees. Glob. Ecol. Biogeogr. 24, 1377–1389. https://doi.org/10.1111/geb.12379.

Vilagrosa, A., Hernández, E.I., Luis, V.C., Cochard, H., Pausas, J.G., 2014. Physiological differences explain the co-existence of different regeneration strategies in Mediterranean ecosystems. New Phytol. 201, 1277–1288. https://doi.org/10.1111/nph.12584.

Wang, R., Gamon, J.A., 2019. Remote sensing of terrestrial plant biodiversity. Remote Sens. Environ. 231, 111218. https://doi.org/10.1016/j.rse.2019.111218.

Wang, Z., Townsend, P.A., Schweiger, A.K., Couture, J.J., Singh, A., Hobbie, S.E., Cavender-Bares, J., 2019. Mapping foliar functional traits and their uncertainties across three years in a grassland experiment. Remote Sens. Environ. 221, 405–416. https://doi.org/10.1016/j.rse.2018.11.016.

Wang, Z., Wang, T., Darvishzadeh, R., Skidmore, A.K., Jones, S., Suarez, L., Woodgate, W., Heiden, U., Heurich, M., Hearne, J., 2016. Vegetation indices for mapping canopy Foliar nitrogen in a mixed temperate Forest. Remote Sens. 8, 491. https://doi.org/10.3390/rs8060491.

Wasson, A.P., Richards, R.A., Chatrath, R., Misra, S.C., Prasad, S.V.S., Rebetzke, G.J., Kirkegaard, J.A., Christopher, J., Watt, M., 2012. Traits and selection strategies to improve root systems and water uptake in water-limited wheat crops. J. Exp. Bot. 63, 3485–3498. https://doi.org/10.1093/jxb/ers111.

Wieczynski, D.J., Boyle, B., Buzzard, V., Duran, S.M., Henderson, A.N., Hulshof, C.M., Kerkhoff, A.J., McCarthy, M.C., Michaletz, S.T., Swenson, N.G., Asner, G.P., Bentley, L.P., Enquist, B.J., Savage, V.M., 2019. Climate shapes and shifts functional biodiversity in forests worldwide. Proc. Natl. Acad. Sci. 116, 587–592. https://doi.org/10.1073/pnas.1813723116.

Zanaga, D., Van De Kerchove, R., Daems, D., De Keersmaecker, W., Brockmann, C., Kirches, G., Wevers, J., Cartus, O., Santoro, M., Fritz, S., Lesiv, M., Herold, M., Tsendbazar, N.-E., Xu, P., Ramoino, F., Arino, O., 2022. ESA WorldCover 10 m 2021 v200. https://doi.org/10.5281/zenodo.7254221.

Zhang, Y.-W., Wang, T., Guo, Y., Skidmore, A., Zhang, Z., Tang, R., Song, S., Tang, Z., 2022. Estimating community-level plant functional traits in a species-rich Alpine meadow using UAV image spectroscopy. Remote Sens. 14, 3399. https://doi.org/10.3390/rs14143399.

Zhang-Zheng, H., Adu-Bredu, S., Duah-Gyamfi, A., Moore, S., Addo-Danso, S.D., Amissah, L., Valentini, R., Djagbletey, G., Anim-Adjei, K., Quansah, J., Sarpong, B., Owusu-Afriyie, K., Gvozdevaite, A., Tang, M., Ruiz-Jaen, M.C., Ibrahim, F., Girardin, C.A.J., Rifai, S., Dahlsjö, C.A.L., Riutta, T., Deng, X., Sun, Y., Prentice, I.C., Oliveras Menor, I., Malhi, Y., 2024a. Contrasting carbon cycle along tropical forest aridity gradients in West Africa and Amazonia. Nat. Commun. 15, 3158. https://doi.org/10.1038/s41467-024-47202-x.

Zhang-Zheng, H., Deng, X., Aguirre-Gutiérrez, J., Stocker, B.D., Thomson, E., Ding, R., Adu-Bredu, S., Duah-Gyamfi, A., Gvozdevaite, A., Moore, S., Oliveras Menor, I., Prentice, I.C., Malhi, Y., 2024b. Why models underestimate west african tropical forest primary productivity. Nat. Commun. 15, 9574. https://doi.org/10.1038/s41467-024-53949-0.

Zirbel, C.R., Bassett, T., Grman, E., Brudvig, L.A., 2017. Plant functional traits and environmental conditions shape community assembly and ecosystem functioning during restoration. J. Appl. Ecol. 54, 1070–1079. https://doi.org/10.1111/1365-2664.12885.